chemosensors

MDPI

Review

Multimodal Sensing and Machine Learning for Nondestructive Quality and Safety Assessment of Agricultural Products

Zhecong Yuan, Xindong Wang, Xinxin Wu and Xinai Zhang *

School of Food Science and Engineering, Jiangsu University, Zhenjiang 212013, China
* Correspondence: zhangxinai@ujs.edu.cn

Abstract

The demand for non-destructive evaluation of agricultural products has stimulated the emergence of multimodal sensing technologies capable of integrating diverse quality- and safety-related information. Recent advances in multimodal sensing and machine learning (ML) have enabled intelligent platforms capable of integrating diverse physicochemical, structural, and biochemical information for comprehensive product characterization. This review summarizes the principles, data-processing strategies, and applications of multimodal sensing systems combining machine vision, visible-near-infrared spectroscopy, hyperspectral imaging, Raman and fluorescence techniques, electronic noses, and auxiliary information with ML algorithms. The complementary capabilities of different sensing modalities for evaluating external appearance, internal quality, chemical composition, freshness, spoilage, and safety hazards are discussed. Meanwhile, the roles of conventional ML and deep learning in feature extraction, pattern recognition, and multimodal data fusion are highlighted. Although advanced algorithms and increased data dimensions improve analytical performance, reliable deployment requires robust datasets, effective calibration transfer, model interpretability, uncertainty assessment, and independent validation. Future advances should prioritize self-supervised and few-shot learning, domain adaptation, physics-informed models, lightweight edge intelligence, and standardized benchmarking to improve model reliability, transferability, and scalability. These innovations will facilitate the deployment of intelligent sensing systems from laboratory environments to real-world agricultural quality and safety management.

Keywords: agricultural products; food quality and safety; nondestructive detection; hyperspectral imaging; machine learning

1. Introduction

Agricultural quality and food safety are governed by a complex combination of physicochemical, sensory, and biological attributes that span multiple spatial and temporal scales [1–5]. Consumers and processors typically evaluate visible characteristics, including color, texture, maturity, and external defects, whereas regulators and supply-chain stakeholders must additionally monitor intrinsic quality indicators and safety-related risks, such as pesticide residues, mycotoxins, adulterants, and other contaminants. These attributes differ substantially in their expression mechanisms and detection requirements [6–10]. Some properties are directly accessible from external surfaces, while others are associated with internal tissues, molecular composition, or microbial activities. Moreover, many safety hazards occur at trace levels and exhibit heterogeneous distribution within agricultural

Check for updates

Received: 26 August 2026
Revised: 7 October 2026
Accepted: 14 October 2026
Published: 16 October 2026

Copyright: © 2026 by the authors. Licensee MDPI, Basel, Switzerland. This article is an open access article distributed under the terms and conditions of the Creative Commons Attribution (CC BY) license.

products. Consequently, a single analytical technique is often insufficient for achieving comprehensive, rapid, and reliable assessment of product quality and safety [11].

Conventional reference methods remain indispensable because they provide accurate and traceable measurements of product quality attributes, microbial contamination, and chemical hazards through well-established laboratory-based techniques [12–14], including chromatographic, spectrometric, immunological, and culture-based approaches [15–22]. However, these methods generally involve destructive sampling, complicated sample preparation, specialized reagents and instruments, intensive labor requirements, and relatively long analysis cycles. Their limited sampling capacity also restricts their application for large-scale inspection and real-time process monitoring. In heterogeneous agricultural commodities, destructive sampling strategies may further overlook localized defects, contamination, or quality variations [23–26]. These limitations have driven the development of rapid, non-destructive sensing technologies capable of enabling high-throughput and continuous evaluation throughout production, storage, and distribution chains.

Recent advances in sensor technology, artificial intelligence, and data analytics have promoted a transition from conventional analytical testing toward intelligent sensing systems. Different sensing modalities provide complementary information associated with diverse product characteristics. Machine vision converts surface appearance into measurable color, shape, and texture descriptors [27–31]. Visible-near-infrared spectroscopy (Vis-NIR) enables rapid characterization of agricultural products by capturing spectral signatures associated with their chemical composition and internal structures. Multispectral and hyperspectral imaging (HSI) further integrate spectral and spatial information, allowing visualization of chemical and physical heterogeneity within samples. Raman and surface-enhanced Raman (SERS) scattering provide vibrational fingerprints with higher molecular specificity [32–38]. Fluorescence sensing offers sensitive responses toward endogenous fluorophores and biochemical interactions, whereas electronic noses (E-noses) characterize volatile signatures associated with ripening, spoilage, or contamination. However, the high-dimensional and heterogeneous data generated by these sensing platforms require advanced analytical strategies. Machine learning (ML) and deep learning (DL) approaches have therefore become essential for extracting informative patterns, establishing nonlinear relationships, and converting complex sensor signals into actionable outputs, including classification, quantitative prediction, and anomaly detection [39–42].

The integration of multiple sensing modalities represents an emerging strategy to overcome the limitations of individual sensors by combining complementary information from different physical domains. Compared with single-modal sensing, multimodal systems have the potential to provide more comprehensive characterization, improve robustness against environmental variations, and enhance prediction reliability. Nevertheless, the successful implementation of multimodal sensing requires not only effective data fusion algorithms but also careful consideration of sensor compatibility, information redundancy, model complexity, and practical deployment conditions.

Four key questions guide this review: Q1. Which sensing technologies are appropriate for specific quality and safety targets? Q2. How do ML and DL approaches improve information extraction beyond traditional chemometric methods? Q3. Under what conditions can multimodal fusion enhance analytical robustness, generalization, and reliability? Q4. What are the major barriers preventing laboratory-developed models from being translated into real-world intelligent inspection systems?

Although numerous reviews have summarized individual sensing technologies, specific agricultural commodities, or particular machine learning algorithms, several critical challenges remain insufficiently addressed. Many previous studies emphasize reported prediction accuracy while providing limited discussion of experimental design factors,

including data partition strategies, sample independence, preprocessing leakage, external validation, reference-method uncertainty, and industrial applicability [43,44]. Furthermore, DL is frequently regarded as a universal replacement for traditional chemometric approaches, despite the fact that many agricultural datasets contain limited sample numbers, strong correlations, and insufficient diversity to support reliable model generalization [45,46]. In addition, multimodal sensing studies are often evaluated based on incremental improvements in internal validation performance, while issues such as true information complementarity, robustness under missing modalities, computational cost, and economic feasibility remain underexplored [47–51].

Therefore, this review presents a reliability-oriented perspective on multimodal sensing and ML-based nondestructive assessment of agricultural products (Figure 1). Rather than simply summarizing sensing techniques and algorithms, this review establishes connections between sensing mechanisms, target attributes, data-processing strategies, and intelligent decision-making. The advantages and limitations of conventional ML and DL models under different data conditions are critically analyzed, while multimodal fusion is examined as a strategy requiring scientific validation rather than an assumed improvement. Particular emphasis is placed on model interpretability, uncertainty evaluation, calibration transfer, domain adaptation, and deployment scalability. Through this perspective, the review aims to provide insights into the development of robust, transferable, and practical intelligent sensing platforms for future agricultural quality and safety management.

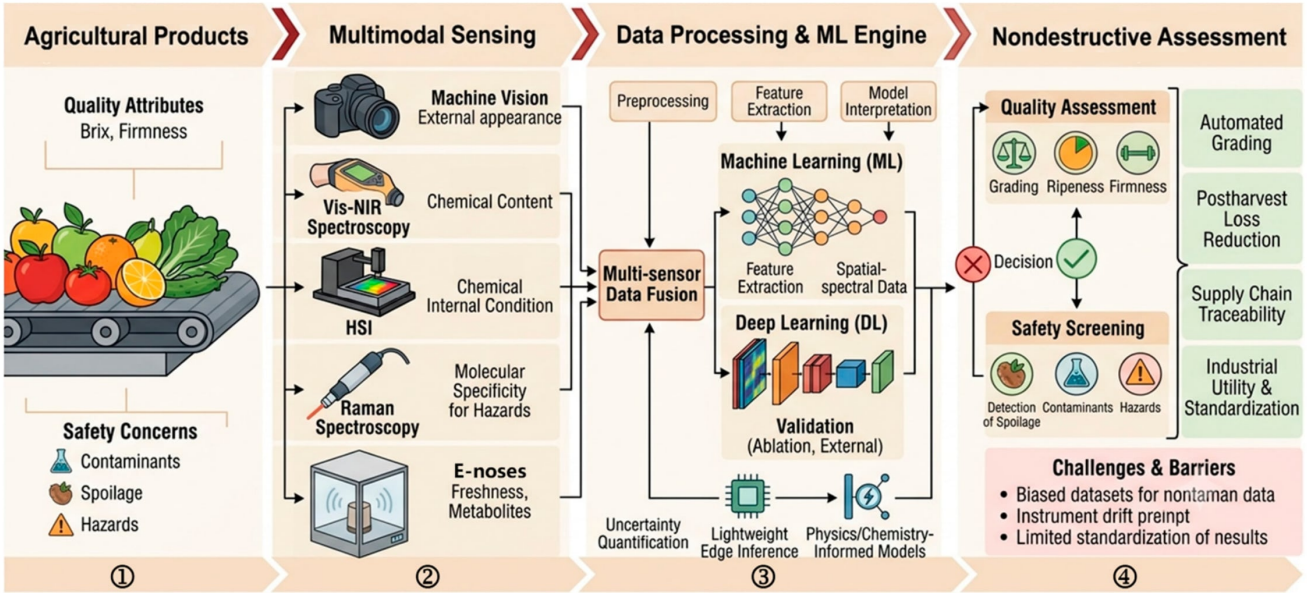


Figure 1. Multimodal sensing and machine learning for nondestructive agricultural product assessment.

2. Analytical Targets as Measurement and Decision Constraints

Rather than treating agricultural quality and safety attributes as a catalogue of measurable indicators, this section classifies analytical targets according to four decision-relevant properties: the causal proximity between the target and the measured signal, the spatial and temporal heterogeneity of the target, the likely sources of confounding, and the level of evidence required for the intended use. A sensing system may be appropriate for rapid grading when it captures a stable surrogate of product quality, but the same system may be insufficient for safety or regulatory decisions when the target is present at trace levels or is only indirectly related to the measured response. This distinction provides the ba-

sis for selecting sensing modalities, modeling strategies, and validation protocols in the following sections.

2.1. External and Internal Quality Attributes

The target of nondestructive inspection should be defined before selecting a sensor or model. External quality includes color uniformity, dimensions, shape, surface roughness, bruising, cracking, insect damage, mold colonies, and other visible defects. These attributes are naturally represented by spatial patterns and are therefore suited to machine vision, multispectral imaging, or hyperspectral classification maps. Internal quality includes water content, soluble solids, acidity, protein, fat, starch, firmness, maturity, internal browning, and tissue breakdown [52–57]. Such properties influence absorption and scattering but may be only indirectly related to the measured optical signal. Their predictability depends on penetration depth, sample geometry, temperature, skin thickness, and the strength of the calibration reference (Table 1).

Table 1. Comparison of major sensing technologies for nondestructive quality and safety assessment of agricultural and food products.

Technology	Information Source	Typical Targets	Advantages	Limitations	Typical Use	Ref.
Machine vision	Spatial patterns: color, texture, shape	Size, color, defects, foreign objects	Low cost, fast, intuitive, simple calibration	Surface information only	Sorting, grading, defect detection	[58]
MSI	Discrete bands (reflectance/emittance) at selected λ	Pigments, moisture, surface defects	Moderate cost, simple calibration	Limited spectral resolution	Sorting, moisture mapping	[59]
HSI	Continuous spectrum for each pixel	Composition, moisture, chemical distribution	Rich information, high spectral resolution	High data volume, complex analysis	Quality prediction, material mapping	[60]
NIR spectroscopy	Molecular overtones and combination absorptions	Moisture, protein, fat, carbohydrates	Fast, robust, minimal sample prep	Overlapping bands, matrix effects	Quality parameters, composition mapping	[61]
Raman/SERS	Molecular vibrational fingerprints	Molecular structure, additives, contaminants	High specificity, structural information	Weak signals, fluorescence interference	Trace contaminants, adulteration	[62, 63]
Fluorescence spectroscopy	Electronic transitions of fluorophores	Spoilage, metabolic products, mycotoxins	Highly sensitive, selective probes	Quenching, background interference	Spoilage detection, mycotoxins	[64]
E-noses	Volatile compounds	Freshness, spoilage, fermentation stage, allergens	Sensitive to volatiles, integrated responses	Cross sensitivity, drift, humidity effects	Freshness grading, spoilage monitoring	[58]
Other biosensing	Biorecognition events	Pathogens, toxins, adulterants	High specificity, potential for field use	Requires labels or surface preparation	Safety screening, rapid detection	[65]

Abbreviations: NIR, near-infrared; SERS, surface-enhanced Raman scattering; E-noses, electronic noses; MSI, multispectral imaging; HSI, hyperspectral imaging.

2.2. Freshness and Spoilage Assessment

Freshness and spoilage represent dynamic quality states resulting from complex physicochemical and biological changes rather than individual measurable analytes. These changes are manifested through alterations in microbial activity, physicochemical prop-

erties, biochemical composition, and sensory characteristics [66–70]. Multimodal sensing approaches integrating spectral, imaging, and gas-sensing information provide opportunities to capture complementary indicators associated with spoilage progression [71–75]. However, freshness prediction models are often established using specific reference parameters and should not be directly interpreted as universal microbial detection systems. Therefore, model validation against independent biological or chemical measurements remains essential for ensuring reliable spoilage assessment.

2.3. Food Safety Hazards and Screening Specificity

Safety assessment requires greater analytical rigor because hazardous factors are often present at low levels, unevenly distributed, and difficult to distinguish from complex sample backgrounds. Conventional spectral approaches may capture indirect variations associated with overall matrix changes rather than the specific hazard itself, leading to potential overestimation of predictive capability [76–80]. Therefore, highly specific sensing strategies based on molecular recognition or targeted signal amplification are often required to improve hazard identification accuracy [81–86]. However, additional procedures involved in these approaches may compromise the principle of strictly nondestructive analysis. Accordingly, intelligent screening systems should be regarded primarily as rapid risk-assessment tools, while regulatory decisions still require confirmation using reliable reference methods.

2.4. Authenticity and Provenance Assessment

Authenticity and provenance assessment aims to verify the identity, origin, and production characteristics of agricultural products by capturing subtle differences in their inherent composition and structural features [87–89]. These tasks often involve complex patterns associated with genetic background, cultivation conditions, processing practices, and supply-chain information. However, authenticity models are particularly susceptible to spurious correlations caused by uncontrolled factors, such as seasonal variations, packaging conditions, instrument differences, or laboratory-specific characteristics. Therefore, high predictive accuracy obtained from randomly partitioned datasets may not necessarily indicate true discrimination capability. Robust model development requires group-aware validation strategies and evaluation using independent origins, production batches, or external datasets to ensure reliable generalization under real-world conditions [90,91].

2.5. Analytical Task Types

Multimodal sensing systems for agricultural assessment generally involve four major analytical task types: classification, regression, localization, and anomaly detection [92–97]. Classification aims to assign samples into predefined categories, whereas regression establishes quantitative relationships between sensor responses and continuous quality or safety attributes. Localization provides spatial information regarding the distribution or severity of defects, while anomaly detection identifies samples that deviate from the characteristics represented in the training dataset. Among these tasks, anomaly detection remains relatively underexplored despite its importance for real-world applications, where systems frequently encounter new varieties, variable storage conditions, unexpected contamination events, or sensor abnormalities [98]. Therefore, reliable deployment requires evaluation beyond closed-set accuracy and should consider model robustness under uncertain and previously unseen scenarios.

3. Intelligent Sensing Technologies and Detection Mechanisms

The development of intelligent nondestructive assessment systems relies on sensing technologies capable of capturing complementary information from different physical and

chemical domains. Individual sensing modalities provide distinct responses related to the external appearance, internal structure, molecular composition, physiological status, and safety characteristics of agricultural products. However, no single sensing technique can simultaneously satisfy the requirements of comprehensive characterization, high sensitivity, rapid analysis, and practical deployment. Therefore, the integration of multiple sensing modalities has emerged as an effective strategy to overcome the limitations of individual approaches by combining complementary signals and improving analytical robustness.

3.1. Machine Vision and Digital Imaging

Conventional red-green-blue imaging (RGB) measures reflected light in broad red, green, and blue bands [99–101]. Its primary information is morphological and colorimetric rather than molecular. After illumination correction and segmentation, images support size measurement, shape analysis, color grading, defect segmentation, and texture characterization [102–105]. The technology is inexpensive, fast, and readily integrated with conveyors. Its main limitation is the inability to detect internal composition or invisible contamination unless these induce external symptoms. Illumination geometry, gloss, shadows, sample orientation, camera exposure, and background strongly affect performance. Color charts and radiometric control are therefore essential when models are expected to transfer between sites.

3.2. Visible-near-Infrared Spectroscopy

Vis-NIR measures reflectance, transmittance, or interactance over wavelength. The visible region contains information from pigments and color-related absorption [106–109]. The near-infrared region is dominated by broad overtone and combination bands of O-H, C-H, and N-H vibrations, making it responsive to water, carbohydrates, proteins, and lipids [110–112]. Scattering carries additional information on tissue microstructure, particle size, porosity, and cellular integrity. Because the bands overlap substantially, multivariate calibration is required [113]. Penetration depends on wavelength, optical geometry, and matrix; interactance and transmittance can probe deeper than simple surface reflectance but often require more controlled hardware. Vis-NIR is well suited to bulk composition, maturity, soluble solids, moisture, protein, fat, and authenticity [114,115]. It is less suitable for trace hazards that do not materially alter the optical matrix. Spectral sensitivity to temperature and path length means that operational control is part of the measurement, not merely a preprocessing issue.

3.3. Multispectral and Hyperspectral Imaging

MSI records a limited number of selected bands [116–118], whereas HSI acquires tens to hundreds of contiguous narrow bands [119–122], producing a three-dimensional data cube with two spatial dimensions and one spectral dimension. The central advantage is simultaneous localization and chemically sensitive contrast. A bruise, fungal colony, foreign material, or region of internal disorder may be mapped rather than represented by a single averaged spectrum [123]. Push-broom systems are common for conveyor inspection, while snapshot systems offer higher temporal resolution at reduced spectral flexibility.

Hyperspectral data are information-rich but operationally expensive. Acquisition generates large files, and spectral redundancy increases computational burden and overfitting risk. Spatial resolution, spectral resolution, signal-to-noise ratio, exposure time, and conveyor speed are coupled engineering choices [124,125]. The most deployable workflow often uses laboratory hyperspectral data to identify informative wavelengths and then implements a lower-cost multispectral device. Deep learning reconstruction of dense spectra from RGB or sparse bands is another emerging route, but reconstructed spectra must

be validated for the downstream task and should not be assumed to preserve chemically meaningful detail [126–129].

3.4. Raman Spectroscopy and Surface-Enhanced Raman Scattering

Raman spectroscopy measures inelastic light scattering associated with molecular vibrations [130–132]. Raman bands are comparatively narrow and chemically interpretable, providing stronger molecular specificity than diffuse near-infrared absorption. Water usually causes less interference than in infrared spectroscopy, which is beneficial for aqueous foods. Raman systems can identify adulterants, additives, pesticides, toxins, and compositional markers [133–135]. Limitations include weak native scattering, fluorescence background, heating, heterogeneous sampling, and sensitivity to focus and surface geometry [136].

SERS amplifies Raman signals near metallic nanostructures and can support trace-level detection. Its analytical value is highest when target capture, substrate uniformity, and spectral classification are controlled. However, substrate batch variation, hotspot heterogeneity, matrix interference, extraction recovery, and reproducibility remain major obstacles [137,138]. Many SERS procedures involve extraction or contact sampling, so the term "nondestructive" should be used carefully. For industrial screening, robust substrates and internal standards may be more important than an increment in model complexity [139–141].

3.5. Fluorescence and Color-Sensor Arrays

Fluorescence sensing measures emitted light after excitation. Signals may arise from intrinsic fluorophores, microbial metabolites, oxidation products, pigments, or target-responsive probes [142–145]. Fluorescence HSI can localize biochemical changes and often offers high sensitivity, but excitation wavelength, photobleaching, quenching, background fluorescence, and matrix opacity affect the response [146–149]. Colorimetric and fluorescent sensor arrays use multiple partially selective sensing elements to create a response pattern [150]. They are attractive for packaging-integrated freshness monitoring and rapid contaminant screening, although shelf life, calibration stability, and environmental cross-sensitivity require careful evaluation.

3.6. Electronic Noses and Volatile Sensing

Electronic noses (E-noses) consist of partially selective gas sensor arrays that generate collective response patterns [151–155], enabling the characterization of volatile fingerprints associated with complex biological and chemical processes. They are particularly suitable for monitoring dynamic changes related to ripening, fermentation, oxidation, spoilage, species identification, and freshness evaluation because these processes produce characteristic variations in headspace composition [156–160]. Unlike chromatographic techniques, E-noses generally provide pattern-based recognition rather than direct identification or quantification of individual volatile compounds. However, their performance can be strongly influenced by environmental conditions, sampling procedures, sensor drift, and signal instability. Therefore, standardized measurement protocols, appropriate calibration strategies, and robust machine learning models are critical for achieving reliable and transferable volatile sensing applications.

3.7. Comparative Interpretation

No sensing modality is intrinsically superior; its value depends on whether the measured signal is causally and operationally linked to the intended decision. RGB imaging is highly deployable for visible defects but cannot provide direct molecular specificity [161]. Vis–NIR spectroscopy is efficient for bulk compositional attributes, yet its broad and

overlapping bands make trace-hazard detection and cross-matrix transfer challenging. Hyperspectral imaging adds spatially resolved chemical contrast, but the resulting gain may be offset by calibration demands, data volume, and throughput limitations [162]. Raman and SERS can provide stronger molecular specificity, although weak signals, substrate variability, matrix interference, or sampling requirements may limit routine deployment [163]. Therefore, sensor selection should begin with the dominant failure mode of the intended application rather than with the nominal analytical capability of the instrument (Table 2).

Table 2. Comparative characteristics of intelligent sensing technologies for agricultural quality and safety assessment.

Technology	Primary Mechanism/ Information	Best-Suited Targets	Main Strengths	Key Limitations	Typical Deployment	Ref.
RGB machine vision	Broadband reflectance; color, morphology, texture	Size, color, shape, surface defects, grading	Low cost, high speed, mature hardware	Surface only; illumination and pose sensitivity	Conveyor grading, smartphone inspection	[58,164]
Vis-NIR	Pigment absorption; O-H, C-H, N-H overtone/ combination bands; scattering	Moisture, soluble solids, protein, fat, maturity	Rapid bulk prediction; compact devices available	Overlapping bands; indirect for trace hazards; matrix dependence	Handheld probes, at-line and in-line monitoring	[61,165]
Multispectral/ HSI	Spatially resolved reflectance or transmittance spectra	Bruises, internal disorders, fungal damage, composition maps, foreign material	Localization plus chemical-sensitive contrast	Large data volume, cost, calibration and speed trade-offs	Laboratory mapping, push-broom sorting, selected-band systems	[166,167]
Raman/SERS	Molecular vibrational fingerprints; plasmon-enhanced scattering for SERS	Adulterants, pesticides, toxins, additives, molecular identity	High specificity; narrow bands; water-compatible	Weak signal, fluorescence, substrate variability, sample-interface demands	Targeted screening, portable confirmation, swab/extract workflows	[137,138, 168]
Fluorescence/ sensor arrays	Intrinsic or probe-mediated emission, quenching and color response	Microbial metabolites, oxidation, toxins, freshness indicators	High sensitivity and imaging compatibility	Photobleaching, background, probe stability, matrix opacity	Packaging indicators, laboratory or portable screening	[142]
E-noses	Pattern of partially selective gas-sensor responses	Ripeness, spoilage, fermentation, species and process differences	Sensitive to headspace dynamics; relatively low cost	Humidity/ temperature effects, drift, indirect specificity	Storage monitoring, freshness screening, process control	[156–158]

Abbreviations: RGB, red-green-blue; Vis-NIR, visible-near-infrared; SERS, surface-enhanced Raman scattering. E-noses, electronic noses; HSI, hyperspectral imaging.

4. From Data Processing to Trustworthy Models

Data processing is not a neutral technical step: each transformation, feature-selection procedure, and model-selection decision can either improve robustness or introduce hidden optimism. The central question is therefore not which algorithm yields the highest internal

score but whether the full analytical pipeline remains stable when the product, batch, instrument, operator, or environment changes.

4.1. Data Preprocessing, Feature Extraction, and Variable Selection

Data preprocessing aims to minimize irrelevant variations while retaining information associated with target attributes [169–171]. For spectral data, commonly applied procedures include reference correction, smoothing, denoising, scatter correction, normalization, baseline adjustment, and derivative transformation. However, each preprocessing strategy introduces specific assumptions and may influence model performance. Therefore, preprocessing procedures should be selected based on nested validation rather than optimized according to final test performance [172–175]. Importantly, all data-dependent operations, including scaling, dimensionality reduction, feature selection, outlier identification, and augmentation parameter estimation, must be performed exclusively within the training folds during resampling [176–178]. Otherwise, information leakage from validation samples may lead to overestimated model performance, particularly in high-dimensional spectroscopic datasets with limited sample sizes.

Image-based analysis requires additional procedures to ensure reliable feature representation, including radiometric correction, background removal, segmentation, region-of-interest extraction, and geometric alignment [179–181]. A critical consideration is maintaining biological independence during dataset construction. Pixel-level samples generated from the same agricultural product are highly correlated and should not be randomly distributed between training and testing sets. Instead, data partitioning should be conducted according to independent units, such as individual samples, batches, fields, or production lots, before pixel extraction. Feature extraction can rely on handcrafted descriptors or data-driven representations [182–185]. While conventional image and spectral features remain useful for interpretation, deep learning models can automatically learn hierarchical patterns from complex multimodal inputs [186–188]. However, dimensionality reduction approaches such as PCA [189] should not be assumed to retain predictive information simply because they explain large variance.

Feature selection and variable optimization are particularly important for high-dimensional sensing systems because they reduce redundancy, alleviate collinearity, and support the development of cost-effective multispectral devices. The robustness of selected variables should be evaluated across repeated validation procedures, as unstable features may reflect sampling variability rather than meaningful relationships. Features consistently identified across different datasets and supported by known physical or chemical mechanisms provide stronger evidence for practical implementation [190]. Data augmentation can further improve model robustness when generated variations represent realistic acquisition conditions [191], such as illumination changes, sensor noise, or spectral fluctuations. Conversely, unrealistic augmentation may introduce artificial patterns unrelated to underlying mechanisms. Class imbalance and abnormal samples should be carefully managed through appropriate sampling strategies, robust evaluation metrics, and mechanistic investigation rather than automatic removal (Figure 2).

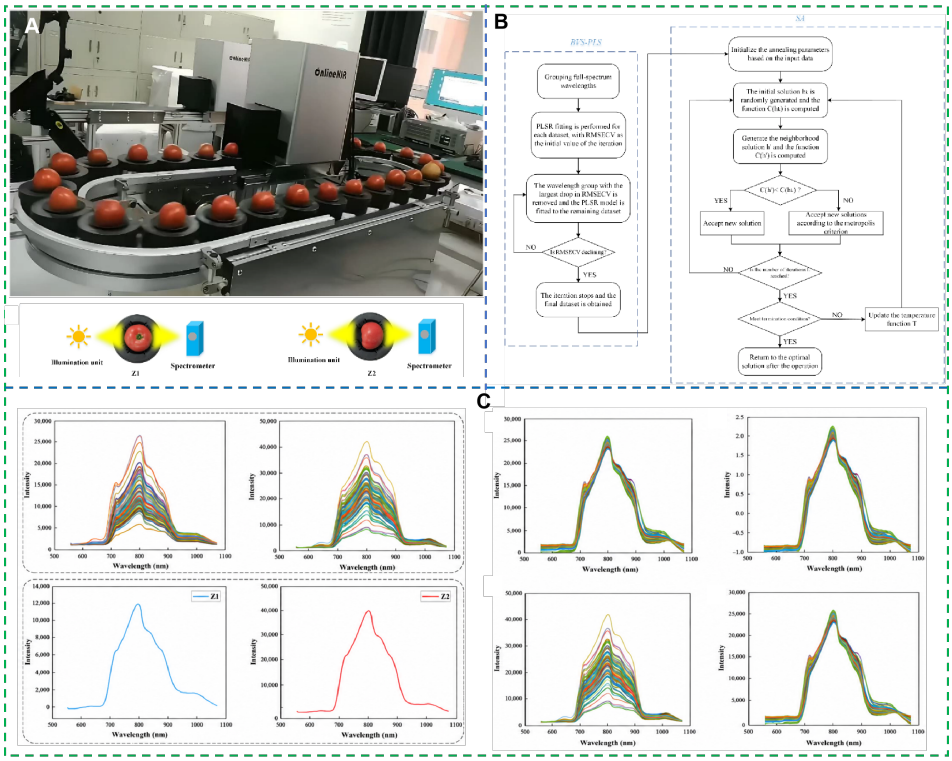


Figure 2. Online full-transmission visible-near-infrared (Vis–NIR) spectroscopy and spectral-modelling workflow for the non-destructive prediction of soluble solids content (SSC) in tomatoes. (**A**) Conveyor-belt-based full-transmission Vis–NIR detection system and two tomato orientations (Z1 and Z2) used for spectral acquisition. (**B**) Wavelength-selection workflows based on backward variable selection–partial least squares (BVS–PLS) and simulated annealing (SA). (**C**) Representative multi-point full-transmission spectra and averaged spectra collected under the two measurement orientations. Adapted from Cai et al. (2024) [192] under the Creative Commons Attribution 4.0 International License (CC BY 4.0).

4.2. Chemometrics and Conventional Machine Learning

Classical chemometrics provides the methodological foundation for many spectral-based agricultural assessments. Principal component analysis (PCA) transforms the original variables into mutually orthogonal principal components ordered by explained variance and is widely used for data visualization, exploratory analysis, dimensionality reduction, and outlier investigation [193]. However, components explaining substantial variance should not be regarded as direct evidence of predictive separability. Partial least-squares regression (PLSR) constructs latent variables by maximizing the covariance between spectral information and target responses, making it particularly suitable for high-dimensional and collinear datasets with limited sample sizes [194]. Its classification counterpart, partial least-squares discriminant analysis (PLS-DA), applies the PLS latent-variable framework to class-coded responses for supervised discrimination. Appropriate calibration of decision thresholds and cautious interpretation of classification probabilities remain important considerations [195].

Conventional machine learning algorithms further extend chemometric analysis by modeling nonlinear relationships and complex feature interactions. Support vector machines (SVMs) identify a maximum-margin separating hyperplane, whereas support vector regression (SVR) extends the regularized kernel-based formulation to continuous responses [196]. Kernel functions enable flexible nonlinear modeling while regularization can reduce overfitting in small- and medium-sized datasets [197,198]. Random forests aggregate predictions from randomized decision trees, while gradients are boosting constructs an additive ensemble by sequentially reducing prediction loss [199]. These approaches

can integrate heterogeneous spectral, image, and metadata features and provide useful variable-importance information; however, their performance and interpretation may be compromised when sample sizes are limited or predictors are highly correlated. Simpler models, such as linear discriminant analysis, logistic regression, and k-nearest neighbors, remain valuable baseline approaches when interpretability and operational transparency are required.

The suitability of conventional models depends strongly on the characteristics of the dataset and analytical objective. For relatively small spectral datasets containing several hundred samples, chemometric methods and traditional machine learning algorithms may achieve comparable or superior performance compared with deep learning approaches [200–204]. However, complex imaging tasks, large-scale multimodal datasets, and spatially resolved analysis often require more advanced representation-learning strategies. Feature engineering remains critical for conventional models [205,206], where physically meaningful preprocessing, stable variable selection, image descriptors, and auxiliary information can improve prediction accuracy while reducing hardware complexity. Nevertheless, extensive feature optimization increases the risk of model-selection bias. Therefore, fair comparisons require consistent data partitioning, leakage-free preprocessing, comparable optimization procedures, and reporting of performance variability rather than only the best-performing results (Figure 3).

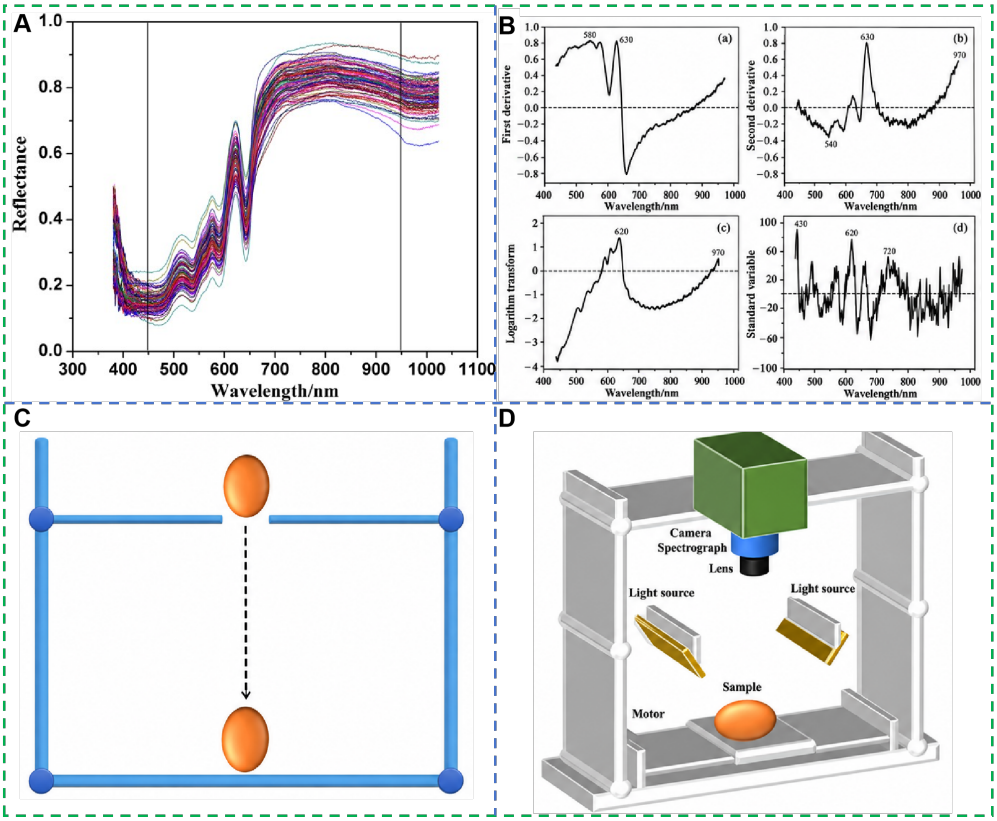


Figure 3. Hyperspectral-imaging setup and spectral analysis for the non-destructive assessment of eggshell quality and crack detection. (**A**) Reflectance spectra of chicken eggs acquired by the hyperspectral imaging system. (**B**) Regression-coefficient profiles and selected characteristic wavelengths for predicting (**a**) L, (**b**) a, (**c**) b color values, and (**d**) eggshell strength. (**C**) Schematic of the impact device used to generate cracked egg samples. (**D**) Line-scan hyperspectral imaging system comprising a camera, imaging spectrograph, lens, dual light sources, and a motor-driven conveyor platform. Adapted from Xie and He [207], Scientific Reports, 2016, licensed under CC BY 4.0.

4.3. Deep Learning for Spectral and Image Analysis

At the methodological level, deep learning models are multilayer differentiable functions trained by back-propagation to minimize a task-specific loss, thereby learning successive representations directly from data rather than relying entirely on manually designed features. Convolutional neural networks use local receptive fields and shared weights to learn repeated spectral or spatial patterns efficiently, which provides the architectural basis for their application to sensing data [208]. For spectral analysis, one-dimensional convolutional neural networks (1D CNNs) treat spectra as sequential signals and automatically extract local absorption and scattering patterns through convolution operations [209–211]. These models can capture nonlinear relationships among neighboring wavelengths and provide efficient end-to-end learning. However, their performance is highly dependent on dataset size and diversity, and insufficient samples may lead to overfitting or the extraction of instrument-specific artifacts rather than meaningful chemical information [212–214].

For image-based sensing, two-dimensional CNNs have been widely applied to RGB images, multispectral data, Raman imaging, and selected-band spectral image [215–217]. By learning hierarchical spatial features, CNNs can effectively characterize appearance variations, structural patterns, and defect-related information. Transfer learning from large image datasets can improve performance when target information is dominated by visual morphology or color characteristics; however, its effectiveness may be limited for spectral representations with statistical properties different from natural images. Three-dimensional CNNs further integrate spatial and spectral dimensions for hyperspectral data analysis, enabling extraction of joint spectral–spatial features [218]. Nevertheless, their computational demands and sensitivity to patch construction require careful experimental design, and specimen-level splitting must be performed before patch generation to prevent information leakage [219,220].

Sequential deep learning architectures, including recurrent neural networks (RNNs), gated recurrent units, and long short-term memory networks, have been explored for spectral interpretation and dynamic quality monitoring [221,222]. Their application is most appropriate when temporal measurements or evolving sensor responses are available, rather than simply relying on the sequential arrangement of wavelength variables. More recently, attention-based architectures and transformers have attracted increasing interest because they can model long-range dependencies that may not be effectively captured by local convolution operations [223,224]. In a transformer, an input spectrum or image is first divided into tokens, such as wavelength intervals for spectral data or image patches for visual data. Each token is projected into query, key, and value representations, and self-attention assigns data-dependent weights to interactions among all tokens. This mechanism enables the model to identify relationships among distant wavelength regions, spatial locations, or spectral–spatial features. Positional information is further incorporated to preserve the sequential order of wavelengths or the spatial arrangement of image patches. Multi-head attention can learn several complementary relationships simultaneously; however, the computational cost increases with token number, and large models may be prone to overfitting when agricultural datasets are limited or insufficiently diverse.

Cross-modal attention extends this principle to multimodal sensing [225]. Rather than simply concatenating features from different sensors, representations from one modality can serve as queries, while representations from another modality provide keys and values. Such a design enables the model to learn which spectral, imaging, volatile-sensing, or metadata features are most relevant to each other for a specific prediction task. Although cross-modal attention can learn latent correspondences between heterogeneous measurements, reliable application still requires rigorous sample-level pairing, temporal synchronization where applicable, modality-specific normalization, and an explicit strategy

for missing or unreliable modalities. Attention weights may support model inspection, but they should not be interpreted as direct causal explanations without further validation using independent chemical, physical, or biological evidence.

Deep generative models provide additional tools for representation learning, denoising, anomaly detection, and data augmentation [226]. An autoencoder contains an encoder that compresses an input signal into a low-dimensional latent representation and a decoder that reconstructs the original input. The reconstruction error can be used to identify atypical spectra or images, while the latent representation can reduce dimensionality before subsequent prediction. A variational autoencoder further models the latent representation as a probability distribution and introduces Kullback–Leibler regularization to obtain a continuous and sampleable latent space [227]. This property can facilitate data generation and uncertainty-aware representation learning; however, reconstructed or generated spectra should be checked carefully to ensure that diagnostically important absorption features and physically meaningful variation are preserved.

Generative adversarial networks learn through competition between a generator, which produces synthetic samples, and a discriminator, which distinguishes synthetic from real samples [228]. Diffusion models instead gradually corrupt real data through a forward noising process and learn a reverse denoising process to generate new samples. These approaches may be useful for class-balanced augmentation, denoising, and simulation of rare but realistic quality or safety conditions. Nevertheless, GANs may suffer from unstable training or limited diversity, whereas diffusion models generally require substantial computational resources [229]. Therefore, synthetic samples should be generated using training data only and evaluated using distributional similarity, preservation of key spectral or image characteristics, class-conditional diversity, and performance improvement on a completely independent real-world test set. Synthetic data should complement, rather than replace, representative experimental measurements.

Overall, the comparison between deep learning and conventional machine learning should consider multiple dimensions rather than accuracy alone (Table 3). DL is particularly advantageous when complex spatial–spectral structures, large-scale data diversity, or multimodal interactions must be modeled. In contrast, conventional approaches may remain preferable for limited datasets, interpretable applications, and resource-constrained deployment scenarios. Therefore, model selection should be guided by data characteristics, analytical objectives, and practical requirements rather than the assumption that increasing model complexity inevitably improves performance.

Table 3. Comparison of chemometric, machine learning, and deep learning model families.

Model Family	Strengths	Weaknesses	Preferred Data Regime	Interpretability/ Deployment	Ref.
PCA/clustering	Exploration, compression, outlier discovery	Unsupervised; variance may not be predictive	Small to medium datasets	High transparency; not a final predictive proof	[230,231]
PLSR/PLS-DA	Handles collinearity; sample efficient; established in spectroscopy	Mostly linear latent structure; threshold calibration needed	Small to medium spectral datasets	Loadings and coefficients aid interpretation; lightweight	[232]
SVM/SVR	Strong nonlinear performance with regularization	Kernel and parameter sensitivity; limited probabilistic output	Small to medium high-dimensional data	Moderate interpretability; feasible on edge devices	[233,234]

Table 3. *Cont.*

Model Family	Strengths	Weaknesses	Preferred Data Regime	Interpretability/ Deployment	Ref.
Random forest/gradient boosting	Nonlinear interactions; mixed features; robust tabular fusion	Can overfit correlated small datasets; importance may be biased	Engineered spectral, image and metadata features	Good deployment profile; explanation tools available	[235]
1D/2D/3D CNN	Automatic local feature learning; spatial or spectral structure	Data and tuning demands; possible shortcut learning	Medium to large structured datasets	Saliency possible; compression often required	[235,236]
RNN/temporal models	Sequential and dynamic signal modeling	Training complexity; often unnecessary for static spectra	Time-series sensing or ordered response curves	Moderate latency and interpretability	[237]
Transformer/cross-attention	Long-range dependencies and flexible multimodal fusion	High data and compute requirements; attention is not explanation	Large or pretrained multimodal datasets	Powerful but deployment and audit are demanding	[238]

Abbreviations: 1D/2D/3D CNN, one-dimensional, two-dimensional and three-dimensional convolutional neural networks; PCA, principal component analysis; PLSR, partial least squares regression; PLS-DA, partial least squares discriminant analysis; SVM, support vector machine; SVR, support vector regression; CNN, convolutional neural network; RNN, recurrent neural network.

5. Multimodal Data Fusion

Multimodal fusion should be treated as a decision-design problem rather than an automatic route to higher accuracy. Before fusion is implemented, the intended decision, the cost of false acceptance and false rejection, the independent information contribution of each modality, and the availability of synchronized measurements should be defined. Fusion is justified only when it improves a decision-relevant property, such as sensitivity to a critical hazard, robustness to environmental variation, uncertainty estimation, or continuity of operation after partial sensor failure. If the additional modality provides only redundant information or introduces unstable batch-related signals, a simpler unimodal system may be preferable [239–241].

5.1. Preconditions for Fusion

Data-level fusion directly integrates raw or minimally processed measurements from multiple sensing sources [242]. Typical examples include combining spectral regions, synchronizing image and spectral signals, or integrating parallel sensor-response streams. This strategy preserves rich original information and allows early discovery of cross-modal relationships. However, successful implementation requires appropriate alignment of sampling scales, temporal synchronization, normalization procedures, and missing-data management. Direct concatenation of high-dimensional measurements may introduce redundancy, increase computational burden, and aggravate overfitting, particularly when sample numbers are limited. Therefore, data-level fusion is most suitable when sensing modalities are physically compatible and sufficient samples are available to support the expanded feature space.

5.2. Selecting the Appropriate Fusion Level

Data-level fusion is most appropriate when modalities are acquired from the same sample under synchronized and physically aligned conditions and when the sample size is

sufficient to support the enlarged input space [243,244]. Feature-level fusion is appropriate when each modality requires independent preprocessing or representation learning, but stable modality-specific features can be extracted and audited before integration. Decision-level fusion is preferable when sensors differ in sampling frequency, data format, reliability, or availability [245,246], because each modality can retain an independent prediction pathway and serve as a fallback when another modality fails. These alternatives should not be regarded as a hierarchy; the appropriate level depends on the measurement architecture and decision requirement.

5.3. Risk-Aligned Error Control and Decision Rules

Decision-level fusion integrates independent model outputs rather than raw measurements or intermediate features. Common strategies include weighted averaging, voting, stacking, Bayesian integration, confidence-based combination, and rule-based decision systems [247,248]. Because each modality is processed separately, this approach provides flexibility when sensors have different acquisition frequencies, formats, or availability. It also improves interpretability by maintaining modality-specific predictions throughout the decision process. However, decision-level fusion may lose fine-grained interactions between modalities that occur at earlier stages of representation learning. In addition, unreliable combination of poorly calibrated probabilities may reduce overall performance, highlighting the importance of confidence estimation and model calibration.

The acceptable error profile must be specified before model optimization. For high-risk safety screening, false-negative risk should be minimized, and uncertain samples should be referred to confirmatory analysis rather than automatically accepted. For grading or sorting, a predefined false-rejection rate may be acceptable when it is justified by product value, throughput, and downstream handling capacity. In all cases, probability calibration, uncertainty estimation, and explicit escalation rules are required before modality outputs are combined into an operational decision.

5.4. Modality Robustness and Fallback Design

Recent advances in attention mechanisms and joint representation learning have enabled deeper integration of heterogeneous sensing information by learning relationships across modalities [249,250]. For example, spectral information can enhance the interpretation of visually ambiguous regions, while volatile signals may provide additional evidence for biochemical changes associated with quality deterioration [251]. Nevertheless, practical multimodal systems must account for variable reliability among sensing sources. Strategies such as modality gating, attention weighting, missing-modality masking, mixture-of-experts architectures, uncertainty estimation, and modality dropout can improve robustness. These mechanisms are particularly important for industrial environments, where sensor contamination, signal saturation, hardware failure, and communication interruptions are unavoidable.

5.5. Verification of Fusion Benefit

Performance improvements after multimodal fusion may originate from different mechanisms and should therefore be interpreted cautiously. A focused comparison of directly comparable studies included in this review illustrates the scale of reported internal fusion gains. For mango-quality classification, the integration of computer vision and a colorimetric sensor array increased prediction accuracy from 92.5% for the best single-modality models to 97.5%[155], corresponding to an absolute gain of 5.0 percentage points [252]. For green-tea-quality classification, multisensory fusion increased prediction accuracy from 78% using the optimal single-sensor information to 92%, corresponding to a gain of 14.0 percentage points. Thus, the directly comparable examples identified in

the reviewed literature showed internal prediction-set gains of 5.0–14.0 percentage points (median: 9.5 percentage points).

These gains should not be interpreted as a pooled estimate of causal complementarity. The two studies differed in commodity, target definition, feature construction, and validation design, and the reported performance was based on prediction sets rather than independent batch, season, or site-level external tests. Consequently, the observed improvement may reflect genuinely complementary information, but it may also be influenced by shared storage or maturity conditions, metadata-related confounding, unequal feature-selection procedures, or differences in model complexity and tuning. Multimodal studies should therefore report the best unimodal comparator, the absolute incremental gain, controlled modality-ablation results, group-aware data partitioning, and external validation before attributing performance improvement to complementary sensing information.

5.6. Deployment Trade-Offs

Multimodal fusion provides the greatest value when individual sensing technologies cannot fully describe the underlying biological or chemical processes (Figure 4). Freshness evaluation represents a typical example, where different sensors capture complementary changes associated with visual appearance, internal composition, biochemical transformation, and volatile evolution [58,253–255]. Similarly, authenticity assessment may benefit from integrating compositional, structural, and contextual information, whereas safety screening may combine rapid broad-spectrum sensing with highly specific confirmation approaches. However, multimodal systems inevitably increase hardware complexity, maintenance requirements, and computational demands. Therefore, fusion should be adopted only when additional information improves decision reliability, robustness, or practical value beyond what can be achieved by a simpler sensing solution.

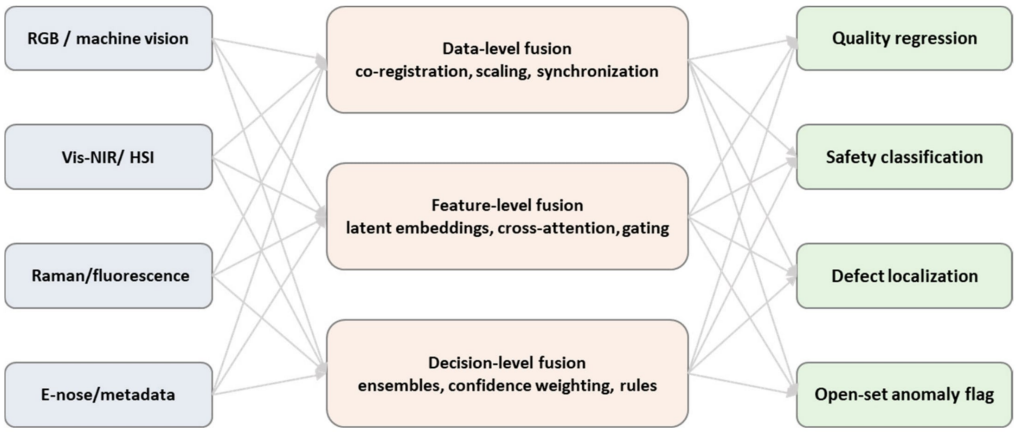


Figure 4. Decision-oriented framework for multimodal fusion: define the analytical objective and error cost, demonstrate complementary information, assess alignment and data sufficiency, select an appropriate fusion level, verify the gain through ablation and external validation, and deploy only when reliability improves beyond a simpler baseline.

6. Representative Applications Across Agricultural Products

6.1. Fruits and Vegetables

Fruits and vegetables represent one of the most extensively investigated commodity groups because their quality characteristics are highly heterogeneous and directly associated with consumer acceptance, processing performance, and economic value [58,256,257]. Imaging-based methods are widely used for external quality evaluation, whereas spectroscopic and hyperspectral approaches provide information related to internal composition, physiological status, and quality deterioration [222,258–260]. Multimodal sensing has

further improved the characterization of complex quality changes by integrating complementary visual, spectral, and biochemical information. However, practical deployment remains challenging due to variations in cultivar, growing environment, seasonal conditions, and postharvest handling. Models developed under controlled laboratory conditions may therefore exhibit limited performance when applied to diverse commercial samples [261,262].

6.2. Grains and Oilseeds

Grains and oilseeds are important targets for nondestructive assessment because their quality is closely related to composition, storage stability, and safety risks [263–268]. Spectroscopic techniques, particularly near-infrared sensing, have been widely adopted for rapid evaluation of bulk properties, while hyperspectral imaging enables spatially resolved inspection and kernel-level classification [269–272]. Machine learning models have shown promise for quality grading, defect recognition, and risk screening. However, safety-related prediction requires careful interpretation because optical responses may reflect indirect changes associated with matrix variation, microbial growth, or physical damage rather than the target hazard itself. Therefore, representative sampling, robust validation, and confirmatory reference analysis remain essential for reliable application.

6.3. Meat and Aquatic Products

Meat and aquatic products require rapid and reliable assessment because their quality changes dynamically during storage and distribution. Multimodal sensing approaches have been applied to evaluate appearance, composition, freshness, authenticity, and spoilage-related changes [127,157,273–276]. Imaging methods provide visual information, while spectroscopy and volatile sensing capture complementary chemical and biochemical variations. However, these products are highly sensitive to environmental and processing conditions, including storage temperature, packaging atmosphere, sample geometry, and measurement protocols [196,277]. Such factors can introduce substantial domain shifts between laboratory datasets and industrial scenarios. Therefore, model development should consider realistic storage conditions and independent validation to ensure reliable transferability.

6.4. Dairy Products, Edible Oils, and Processed Foods

Dairy products, edible oils, and processed foods provide diverse opportunities for nondestructive composition analysis, quality monitoring, and authenticity assessment. Spectroscopic approaches can effectively characterize compositional variations and detect quality changes when target-related signals are sufficiently expressed. Raman and surface-enhanced Raman techniques offer additional molecular specificity for targeted analysis [278–280]. However, processed foods often contain complex matrices involving multiple ingredients, heterogeneous structures, and variable processing histories. Consequently, models developed for one formulation or production condition may not generalize well across different brands, raw materials, particle structures, or manufacturing processes. Reliable deployment requires evaluation of matrix effects and validation across diverse real-world samples.

6.5. Tea, Medicinal Plants, Spices, and Specialty Products

Tea, medicinal plants, spices, and other specialty products are frequently investigated for authenticity, origin verification, quality grading, and processing characterization. Their complex chemical compositions generate characteristic spectral and volatile patterns that can support discrimination among different product categories [165,166,281–289]. However, provenance-related models are particularly vulnerable to confounding factors, including

harvest season, supplier differences, storage conditions, and instrumental variation. High classification accuracy obtained from randomly divided datasets may therefore overestimate true geographical or biological discrimination capability.

A worked example can clarify this risk. Consider a tea-origin dataset containing samples from three geographical regions, with four independent harvest lots per region and multiple spectra acquired from each lot [290]. If the spectra are randomly divided at the spectrum level, measurements from the same harvest lot may occur in both the training and test sets. The resulting accuracy then evaluates recognition of another spectrum from an already represented lot, rather than provenance discrimination for a new harvest lot. A more appropriate design assigns all spectra from each lot to a single partition and holds out complete lots, while retaining each geographical class in the training data. Where possible, the held-out groups should also represent different seasons, suppliers, or acquisition sites.

The practical consequence of this distinction has been demonstrated in a related Vis–NIR agricultural sensing study. Egg-level stratified five-fold validation produced an accuracy of 0.915 ± 0.015, whereas leave-one-incubation-batch-out validation yielded 0.846 ± 0.014, corresponding to an absolute decrease of 6.9 percentage points [291,292]. This comparison does not itself demonstrate data leakage, because measurements from the same egg were kept within one partition; rather, it quantifies the performance reduction that can arise when a model is evaluated on a previously unseen batch. Accordingly, reliable authenticity assessment should report group-wise or prospective validation results in addition to random or within-group validation.

6.6. Cross-Commodity Matrix Effects and Transferability

Despite successful demonstrations across various agricultural products, transferability remains a major challenge for intelligent sensing systems. Matrix characteristics influence signal generation and model performance through variations in composition, structure, morphology, and environmental conditions. Factors such as water distribution, particle characteristics, surface properties, and temperature-dependent responses can alter spectral, imaging, and volatile signals. Therefore, models should not be assumed to be universally transferable across commodities or application scenarios without sufficient evidence. Establishing robust calibration strategies, domain adaptation methods, and independent validation protocols is essential for achieving reliable cross-matrix deployment (Table 4).

Table 4. Representative application matrix linking products, targets, sensing combinations, and generalization risks.

Product Matrix	Representative Targets	Suitable Sensing Combinations	Modeling Emphasis	Generalization Risk	Ref.
Fruits and vegetables	Maturity, soluble solids, firmness, bruises, disease	RGB + Vis-NIR/HSI; optional fluorescence	Spatial-spectral regression and defect segmentation	Cultivar, season, orchard, temperature, skin thickness	[293–295]
Grains and oilseeds	Moisture, protein, fungal damage, mycotoxin risk, foreign material	NIR + HSI; Raman/SERS for targeted hazards	Kernel-level classification; bulk calibration; anomaly detection	Lot, cultivar, storage, uneven contamination	[296–298]
Meat and aquatic products	Freshness, oxidation, fat, tenderness, microbial spoilage	RGB/HSI + fluorescence + E-noses	Multimodal temporal prediction and confidence-based screening	Packaging atmosphere, cut geometry, temperature, headspace protocol	[299–301]

Table 4. *Cont.*

Product Matrix	Representative Targets	Suitable Sensing Combinations	Modeling Emphasis	Generalization Risk	Ref.
Milk, dairy, oils and processed foods	Composition, adulteration, oxidation, process state	NIR/Raman + imaging + metadata	Nonlinear regression, authenticity classification, transfer learning	Brand, formulation, particle size, processing conditions	[302–304]
Tea, herbs, spices and specialty products	Origin, variety, grade, processing, adulteration	NIR/HSI + E-noses + metadata	Domain-aware classification and open-set recognition	Harvest year, supplier, packaging, provenance confounding	[305–307]

Abbreviations: RGB, red-green-blue; Vis-NIR, visible-near-infrared; SERS, surface-enhanced Raman scattering. E-noses, electronic noses; HSI, hyperspectral imaging.

7. Model Reliability, Industrial Translation, Challenges, and Future Directions

7.1. Model Evaluation, Explainability, and Reliability

Reliable evaluation is fundamental for determining whether machine learning models can generalize beyond experimental datasets. Appropriate performance assessment should consider the analytical task, data distribution, and practical decision requirements rather than relying solely on overall accuracy. Classification studies should include class-specific metrics, confusion matrices, and imbalance-aware indicators, whereas regression models should report complementary measures such as prediction error and explained variance [308,309]. Data partitioning strategies must reflect the actual deployment scenario [310,311]. Samples originating from the same biological source, production batch, or environmental condition should remain within the same data partition to avoid information leakage. Random splitting may substantially overestimate performance when hidden group effects dominate [312]. Therefore, independent test sets, nested validation strategies, and external evaluations are essential for assessing true model generalization.

External validation provides a more realistic assessment of robustness by introducing variations in season, origin, operator, instrument, and production conditions. Such evaluation is particularly important for agricultural products because biological variability can arise from environmental factors, cultivation practices, and storage history [313]. When performance degradation occurs, recalibration should not be performed directly on the test set but should be quantified and analyzed. Calibration transfer methods, including standardization approaches, spectral augmentation, representation alignment, and transfer learning, can improve model adaptation across different acquisition conditions [314,315]. However, transfer strategies should be evaluated against appropriate baselines and should clearly report the amount and type of additional data required for successful adaptation.

Beyond accuracy, uncertainty estimation and interpretability are essential for safe deployment. Industrial sensing systems should quantify prediction confidence and recognize samples outside the model's reliable operating range. Methods including ensemble learning, Bayesian approximation, conformal prediction, and out-of-distribution detection provide potential solutions for estimating different sources of uncertainty [316]. Explainable artificial intelligence approaches can further improve model transparency by identifying influential features, spectral regions, or image areas [317]. However, explanations should be validated for stability, reproducibility, and consistency with known physical mechanisms. Attention maps or visual explanations alone should not be interpreted as direct evidence of causal relationships, particularly in highly correlated spectral datasets [318].

Reproducible research practices are necessary to accelerate translation from laboratory models to practical systems. Comprehensive reporting should include sample characteristics, reference methods, sensor configurations, acquisition conditions, preprocessing procedures, data partition strategies, augmentation methods, model architectures, optimization procedures, and computational settings. Reporting only the highest-performing model among multiple trials may introduce selection bias and limit reproducibility [319,320]. Whenever possible, sharing raw signals, metadata, trained models, and external evaluation results can facilitate independent verification and improve confidence in model reliability (Table 5).

Table 5. Minimum and preferred practices for reliable model development and reporting.

Reliability Item	Minimum Acceptable Practice	Preferred High-Rigor Practice	Ref.
Sampling unit	Split by independent sample	Split by batch/site/season and retain a prospective set	[308,309]
Preprocessing	Fit transformations on training data only	Use a fully nested pipeline with locked external test data	[310–312]
Model comparison	Same partitions and metrics	Same inputs, tuning budget, seeds, uncertainty and computer reporting	[313]
Classification metrics	Accuracy plus class-wise sensitivity/recall	Balanced accuracy, MCC, PR-AUC, calibration and decision-cost analysis	[314,315]
Regression metrics	RMSE/MAE and R^2	Bias, slope, residual plots, prediction intervals and application thresholds	[316]
External validation	Independent production batch	Cross-season, cross-origin, cross-instrument and multisite validation	[317]
Explainability	Feature or region attribution	Stability tests, perturbation tests and physical/chemical consistency	[318]
Reproducibility	Complete methods and hyperparameters	Code, raw data, metadata, trained model and external predictions	[319,320]

Abbreviations: MCC, Matthews correlation coefficient; PR-AUC, area under the precision–recall curve; RMSE, root mean square error; MAE, mean absolute error; R^2, coefficient of determination.

7.2. From Laboratory Models to Practical Equipment

The transition from laboratory-based models to practical sensing systems requires simultaneous consideration of hardware adaptation, computational efficiency, and operational reliability. Portable and handheld platforms, including compact spectrometers, smartphone-based imaging systems, and miniaturized sensor arrays, provide opportunities for field, warehouse, and on-site inspection applications. However, miniaturization inevitably alters optical configuration, spectral resolution, signal quality, and calibration stability. Therefore, laboratory-developed models cannot be directly transferred to portable devices without evaluating instrument differences and applying appropriate calibration or transfer strategies [321–326]. Successful deployment requires optimization of both sensing hardware and analytical models according to the intended application scenario.

Online inspection and automated sorting impose additional requirements beyond prediction accuracy. Industrial systems must integrate sensing, data processing, sample tracking, and mechanical decision-making within limited time windows. Factors such as acquisition speed, processing latency, false acceptance, false rejection, maintenance requirements, and system throughput are equally important for practical performance [327]. Edge computing and lightweight artificial intelligence can reduce computational demands through model compression, pruning, quantization, knowledge distillation, and compact

architectures [328]. A promising strategy is to use high-dimensional sensing platforms for initial information discovery, followed by identification of essential features and development of simplified sensors optimized for real-time decisions [329].

From an industrial engineering standpoint, deployment feasibility is tightly governed by capital expenditure (CapEx), recurring operational/maintenance expenses (OpEx), and line inspection throughput. In commercial conveyor-sorting operations (e.g., fruit and vegetable packing lines), sorting rates typically demand processing speeds between 5 to 15 items per second (or conveyor velocities of 0.5–2.0 m/s) with per-item inference latencies strictly below 30–50 ms [330].

Single-modality machine vision systems operating in the visible domain represent the lowest economic threshold and effortlessly achieve sorting throughputs exceeding 10–20 items/s [331]. Point-scan Vis–NIR spectrometers fall into a moderate price regime and can acquire integration spectra within 10–100 ms, making them viable for high-speed online grading [332].

In contrast, push-broom hyperspectral imaging (HSI) systems, while providing chemical and spatial distribution maps, incur substantially higher hardware investments. Furthermore, due to multi-band exposure times and massive data cube serialization (often generating hundreds of megabytes per second), full-band HSI typically operates at restricted speeds of 1–3 items/s, falling short of high-speed industrial conveyor demands unless paired with stable characteristic band selection down to multispectral setups [333].

Gas-sensing arrays (E-noses) and colorimetric arrays face a different bottleneck: while sensor component costs are low, chamber dead-volume equilibration and sensor baseline recovery impose typical acquisition cycles of 30 s to 5 min per measurement, rendering them unsuitable for continuous in-line conveyor sorting and restricting their economic deployment to batch storage monitoring, headspace warehouse surveillance, or at-line QA screening. Therefore, multimodal fusion must be quantitatively evaluated by the marginal accuracy/safety benefit per dollar of added sensor cost and per millisecond of added latency.

Long-term operation requires robustness against environmental variability and regulatory constraints. Factors such as illumination changes, temperature, humidity, vibration, contamination, and sample positioning can introduce signal drift and reduce model reliability. Therefore, practical devices should incorporate calibration standards, quality-control procedures, environmental compensation, and continuous monitoring mechanisms to identify sensor degradation or out-of-distribution samples. Furthermore, commercial and regulatory acceptance depends on traceability to reference methods, quantified uncertainty, documented maintenance procedures, and clearly defined application boundaries. Validation should therefore match the intended purpose, whether grading, process monitoring, screening, or regulatory decision-making, and performance claims should remain consistent with available evidence (Table 6).

Table 6. Principal barriers to industrial translation and corresponding technical priorities.

Translation Barrier	Operational Consequence	Priority Solution	Ref.
Instrument and batch drift	Calibration decay and unstable thresholds	Transfer standards, invariant representations, drift alarms and scheduled maintenance	[334,335]
Environmental variation	False rejects/accepts under light, temperature or humidity changes	Shielding, reference correction, compensation models and stress testing	[336,337]

Table 6. *Cont.*

Translation Barrier	Operational Consequence	Priority Solution	Ref.
Large hyperspectral data	Latency, storage and hardware cost	Stable wavelength selection, multispectral redesign, compression and edge acceleration	[338]
Weak hazard specificity	Risk of confusing indirect matrix effects with contaminants	Target-specific Raman/SERS/biosensing and confirmatory reference analysis	[339]
Missing or failed modalities	Multimodal model cannot produce a decision	Modality dropout, reliability gating, fallback unimodal models and sensor diagnostics	[339,340]
Uncertain predictions	Unsafe automated decisions	Calibrated confidence, conformal prediction, abstention and human/reference escalation	[341]
Lack of standards and traceability	Low regulatory and commercial acceptance	Intended-use validation, reference-method traceability, uncertainty budgets and reporting standards	[342]

7.3. Evidence-Based Barriers to Reliable Translation

A first barrier is the mismatch between experimental datasets and the population encountered after deployment. Agricultural sensing datasets are frequently small, homogeneous, and structured by product batch, season, cultivar, instrument, operator, or storage condition. Random sample-level splitting can therefore produce optimistic internal estimates when correlated measurements from the same independent unit are represented in both training and test sets. The practical consequence of validation design has been demonstrated in a Vis–NIR study of 1600 eggs from four incubation batches: egg-level five-fold validation achieved an accuracy of 0.915 ± 0.015, whereas leave-one-batch-out validation yielded 0.846 ± 0.014 [291]. This difference does not by itself prove data leakage because individual eggs were kept within one partition; however, it quantifies the reduction in performance that can occur when a model is evaluated on a previously unseen batch.

A second barrier is measurement transfer. A model may perform well with one instrument configuration yet fail to transfer directly to another device or laboratory because of wavelength shifts, optical geometry, detector response, sample presentation, or environmental variation. In a multi-instrument study of edible-oil authenticity screening, inter-instrument differences were sufficient to compromise direct transfer of classification models developed using raw low-field NMR data [343]. This finding illustrates why calibration transfer, reference standards, and cross-instrument validation must be treated as part of the analytical method rather than as optional post-processing steps.

A third barrier concerns analytical specificity and the quality of the reference method. Broad spectral or volatile fingerprints may correlate with a hazard-associated matrix change without directly measuring the hazard itself. This problem is especially important for trace contaminants, complex food matrices, and safety decisions with asymmetric false-negative risk. Targeted SERS approaches can improve molecular specificity, but practical implementation remains limited by substrate reproducibility, nonspecific binding, matrix interference, and incomplete standardization [344]. Therefore, high laboratory sensitivity should not be interpreted as sufficient evidence for routine screening unless selectivity, reproducibility, recovery, and comparison with an independent reference method are demonstrated.

A fourth barrier is operational integration. A deployable system must maintain traceable sample handling, stable acquisition, calibration control, data integrity, model monitoring, latency-compatible inference, and defined action rules over extended operation [345]. A highly accurate laboratory model may still be unsuitable for industrial use if it cannot identify sensor drift, missing modalities, out-of-distribution samples, or uncertain predictions. Reliable translation therefore requires co-design of the sensor, reference method, model, quality-control procedure, maintenance plan, and human or confirmatory escalation pathway.

Addressing these barriers requires solution pathways that are matched to their underlying causes. Dataset–deployment mismatch should be addressed through representative sampling across batches, seasons, sites, and instruments, together with group-aware and prospective validation; the trade-off is greater experimental cost and longer data-collection cycles, which should be justified by improved external performance. Instrument and environmental drift require reference standards, calibration transfer, drift monitoring, and scheduled recalibration, but these measures increase maintenance requirements and depend on the availability of representative transfer samples. Weak analytical specificity should be addressed through targeted sensing strategies and confirmatory reference analysis; however, greater specificity may reduce throughput, increase cost, or compromise strictly nondestructive operation. For multimodal systems, reliability gating, unimodal fallback models, and sensor diagnostics can mitigate missing or failed modalities, although they increase system and validation complexity. Finally, calibrated uncertainty estimation, abstention rules, and human or reference-method escalation can reduce unsafe automated decisions, but they necessarily increase the proportion of samples requiring secondary assessment. The effectiveness of these measures should be verified using cross-domain validation, environmental stress testing, reference-method agreement, calibration analysis, and explicit monitoring of false-negative risk.

7.4. Priority Research Directions for Overcoming Identified Barriers

Future research should be prioritized according to the barriers identified above rather than according to algorithmic novelty alone. The first and most fundamental priority is the establishment of representative datasets, traceable reference measurements, and group-aware external validation protocols. These elements address dataset–deployment mismatch, label uncertainty, and hidden batch effects; without them, improvements in model architecture cannot be interpreted as reliable progress.

The second priority is robust measurement transfer and risk-aware model operation. Calibration transfer, environmental compensation, drift monitoring, uncertainty estimation, and out-of-distribution detection should be integrated into model development from the outset. These strategies directly address the loss of performance caused by instrument differences, changing acquisition conditions, and previously unseen samples. Their success should be assessed through cross-batch, cross-season, cross-instrument, and prospective validation rather than internal accuracy alone.

The third priority is reliability-aware multimodal and deployable system design. Multimodal fusion should be introduced only when complementary information has been demonstrated and when the added modality improves a decision-relevant property, such as sensitivity, robustness, uncertainty reduction, or fault tolerance. Lightweight models, selected-band sensors, and edge implementation are then required to balance analytical performance against throughput, maintenance, cost, and latency. Advanced methods, including self-supervised learning, transformers, and generative models, should be evaluated as enabling tools for these three priorities rather than as independent objectives.

Future research should therefore evaluate each proposed advance not only by its improvement in internal predictive performance, but also by the deployment barrier it addresses, the additional resources it requires, and the evidence demonstrating that its benefit is retained under realistic operating conditions.

8. Conclusions

Intelligent sensing integrated with machine learning provides a powerful framework for rapid, non-destructive, and comprehensive assessment of agricultural quality and safety. While conventional chemometric approaches remain highly effective for small-scale and high-dimensional spectral datasets, deep learning offers additional advantages for complex imaging tasks, large heterogeneous datasets, and multimodal representation learning. Multimodal fusion has the potential to enhance analytical performance and robustness by integrating complementary information across sensing modalities, but its success depends on appropriate data alignment, reliable validation, uncertainty assessment, and practical cost considerations. Future progress should move beyond maximizing laboratory accuracy toward developing trustworthy sensing systems characterized by robust generalization, interpretability, transferability, and operational stability. Achieving this goal requires coordinated advances in data quality, model evaluation, sensor engineering, and hardware–software integration to enable reliable deployment under diverse real-world agricultural conditions.

Author Contributions: Z.Y., as the leading author handled Writing—original draft preparation and completed the review. X.W. (Xindong Wang) reviewed literature citations; X.W. (Xinxin Wu) evaluated argument logic. X.Z. did Writing—review and editing, revised key sections, and took charge of Supervision. All authors have read and agreed to the published version of the manuscript.

Funding: This research received no external funding.

Institutional Review Board Statement: Not applicable.

Informed Consent Statement: Not applicable.

Data Availability Statement: No new data were created or analyzed in this study. Data sharing is not applicable to this article.

Acknowledgments: During the preparation of this manuscript, the authors used GPT-5.3 Instant solely to improve the readability, sentence structure, and linguistic clarity of selected passages. The authors critically reviewed and edited all AI-assisted text, developed and evaluated the scientific content, and take full responsibility for the accuracy, integrity, originality, and final content of the manuscript.

Conflicts of Interest: The authors declare no conflicts of interest.

References

1. Du, Z.; Hu, Y.; Buttar, N.; Mahmood, A. X-ray computed tomography for quality inspection of agricultural products: A review. *Food Sci. Nutr.* **2019**, *7*, 3146–3160. [CrossRef] [PubMed]
2. Cheng, J.; Yu, P.; Huang, Y.; Zhang, G.; Lu, C.; Jiang, X. Application Status and Prospect of Impedance Spectroscopy in Agricultural Product Quality Detection. *Agriculture* **2022**, *12*, 1525. [CrossRef]
3. Kutsanedzie, F.; Guo, Z.; Chen, Q. Advances in Nondestructive Methods for Meat Quality and Safety Monitoring. *Food Rev. Int.* **2019**, *35*, 536–562. [CrossRef]
4. Zhang, C.; Li, X.; Yan, H.; Ullah, I.; Zuo, Z.; Li, L.; Yu, J. Effects of irrigation quantity and biochar on soil physical properties, growth characteristics, yield and quality of greenhouse tomato. *Agric. Water Manag.* **2020**, *241*, 106263. [CrossRef]
5. Ali, M.; Hashim, N.; Abd Aziz, S.; Lasekan, O. Principles and recent advances in electronic nose for quality inspection of agricultural and food products. *Trends Food Sci. Technol.* **2020**, *99*, 1–10. [CrossRef]
6. Li, Y.; Wang, Y.; Fan, L.; Wang, F.; Liu, X.; Zhang, H.; Zhou, J. Assessment of β-D-glucosidase activity and *bgl* gene expression of *Oenococcus oeni* SD-2a. *PLoS ONE* **2020**, *15*, e0240484. [CrossRef] [PubMed]

7. Yin, H.; Hu, X.; Huang, X.; Zou, X.; Xu, Y.; Shi, J.; Yang, M. Rapid Discrimination of Beer Flavors Using Ion-Selective Electrode Array System Combined with Chemometrics. *Food Anal. Methods* **2021**, *14*, 1836–1842. [CrossRef]
8. Li, H.; Sheng, W.; Haruna, S.; Hassan, M.; Chen, Q. Recent advances in rare earth ion-doped upconversion nanomaterials: From design to their applications in food safety analysis. *Compr. Rev. Food Sci. Food Saf.* **2023**, *22*, 3732–3764. [CrossRef] [PubMed]
9. Deng, S.; Wu, X.; Shi, Y.; El-Mesery, H.; Zhang, X. Uncovering Analytical Patterns for Hazardous Components in Agricultural Production Systems. *Foods* **2025**, *14*, 3261. [CrossRef] [PubMed]
10. Zhou, J.; Zou, X.; Song, S.; Chen, G. Quantum Dots Applied to Methodology on Detection of Pesticide and Veterinary Drug Residues. *J. Agric. Food. Chem.* **2018**, *66*, 1307–1319. [CrossRef] [PubMed]
11. Singh, R.; Zhang, W.; Liu, X.; Zhang, B.; Kumar, S. WaveFlex Biosensor: MXene-Immobilized W-shaped Fiber-Based LSPR sensor for highly selective tyramine detection. *Opt. Laser Technol.* **2024**, *171*, 110357. [CrossRef]
12. Zhang, H.; Mahunu, G.; Castoria, R.; Yang, Q.; Apaliya, M. Recent developments in the enhancement of some postharvest biocontrol agents with unconventional chemicals compounds. *Trends Food Sci. Technol.* **2018**, *78*, 180–187. [CrossRef]
13. Okeke, E.; Ezeorba, T.; Okoye, C.; Chen, Y.; Mao, G.; Feng, W.; Wu, X. Analytical detection methods for azo dyes: A focus on comparative limitations and prospects of bio-sensing and electrochemical nano-detection. *J. Food Compos. Anal.* **2022**, *114*, 104778. [CrossRef]
14. Su, X.; Chen, Z.; Wang, H.; Yuan, L.; Zheng, K.; Zhang, W.; Zou, X. Ratiometric immunosensor with DNA tetrahedron nanostructure as high-performance carrier of reference signal and its applications in selective phoxim determination for vegetables. *Food Chem.* **2022**, *383*, 132445. [CrossRef] [PubMed]
15. Mustapha, A.; Zhou, C.; Amanor-Atiemoh, R.; Ali, T.; Wahia, H.; Ma, H.; Sun, Y. Efficacy of dual-frequency ultrasound and sanitizers washing treatments on quality retention of cherry tomato. *Innov. Food Sci. Emerg. Technol.* **2020**, *62*, 102348. [CrossRef]
16. Hassan, M.; Yi, X.; Zareef, M.; Li, H.; Chen, Q. Recent advancements of optical, electrochemical, and photoelectrochemical transducer-based microfluidic devices for pesticide and mycotoxins in food and water. *Trends Food Sci. Technol.* **2023**, *142*, 104230. [CrossRef]
17. Gao, R.; Liu, H.; Li, Y.; Liu, H.; Zhou, Y.; Yuan, L. Correlation between dominant bacterial community and non-volatile organic compounds during the fermentation of shrimp sauces. *Food Sci. Hum. Wellness* **2023**, *12*, 233–241. [CrossRef]
18. Yan, J.; Cai, W.; Wang, C.; Yu, Y.; Zhang, H.; Yang, Y.; Wang, W. Macromolecular behavior, structural characteristics and rheological properties of alkali-neutralization curdlan at different concentrations. *Food Hydrocoll.* **2020**, *105*, 105785. [CrossRef]
19. Dong, Z.; Lu, J.; Wu, Y.; Meng, M.; Yu, C.; Sun, C.; Chen, M.; Da, Z.; Yan, Y. Antifouling molecularly imprinted membranes for pretreatment of milk samples: Selective separation and detection of lincomycin. *Food Chem.* **2020**, *333*, 127477. [CrossRef] [PubMed]
20. Li, Q.; Li, C.; Li, E.; Gilbert, R.; Xu, B. A molecular explanation of wheat starch physicochemical properties related to noodle eating quality. *Food Hydrocoll.* **2020**, *108*, 106035. [CrossRef]
21. Gao, R.; Yu, Q.; Shen, Y.; Chu, Q.; Chen, G.; Fen, S.; Yang, M.; Yuan, L.; McClements, D.; Sun, Q. Production, bioactive properties, and potential applications of fish protein hydrolysates: Developments and challenges. *Trends Food Sci. Technol.* **2021**, *110*, 687–699. [CrossRef]
22. Jiang, W.; Zhu, W.; Yang, Q.; Wu, W.; Hou, X. An electrochemical/colorimetric dual-mode sensor for the detection of AFB1 in agricultural products based on CoFe2O4@Au nanoparticles and smartphone imaging. *Food Chem.* **2025**, *474*, 143201. [CrossRef] [PubMed]
23. Khulal, U.; Zhao, J.; Hu, W.; Chen, Q. Nondestructive quantifying total volatile basic nitrogen (TVB-N) content in chicken using hyperspectral imaging (HSI) technique combined with different data dimension reduction algorithms. *Food Chem.* **2016**, *197*, 1191–1199. [CrossRef] [PubMed]
24. Tian, X.; Fang, Q.; Dong, H.; Zhang, X.; Aheto, J.; Bai, J. Visualizing bolus development using hyperspectral imaging: Effects of buckwheat substitution on the oral processing of Chinese steamed bread. *J. Cereal Sci.* **2026**, *128*, 104411. [CrossRef]
25. Xu, A.; Gao, J.; Li, H.; Song, X.Y.; Xu, B.; Liu, Y.; Yu, Y.Y.; Wang, P.; Wang, Q.; Zhou, M. High-Voltage aqueous supercapacitors based on l-lysine pH Self-Buffering Coating-modified carbon cloth electrode. *Chem. Eng. J.* **2025**, *509*, 161289. [CrossRef]
26. Sun, Q.; Yuan, Y.; Zhang, M.; Xu, F.; Guo, Z.; Wang, X.; Ren, J.; Shi, J.; Zou, X. An Innovative Color Control Strategy of Fruits and Vegetables During Drying. *Food Bioprocess Technol.* **2025**, *18*, 8686–8701. [CrossRef]
27. Lu, S.; Zhao, J.; Qin, Q.; Deng, W.; Yu, Y.; Huang, Y.; Li, M.; Dong, H.; Li, Z. Identification of roasting degree and interpretability analysis of Yunnan arabica coffee beans based on multi-dimensional visual features and CNNs-SHAP. *Food Chem.* **2026**, *508*, 148367. [CrossRef] [PubMed]
28. Hassan, M.; Xu, Y.; Sayada, J.; Zareef, M.; Jiao, T.; Chen, M.; Chen, X.; Li, H.; Chen, Q. Trends in smart surface-enhanced Raman scattering sensors for food hazards. *Trends Food Sci. Technol.* **2025**, *163*, 105199. [CrossRef]
29. Mei, C.; Zhu, J.; Zhu, W.; Wang, H.; Jiang, H. Combining Colorimetric Sensor Technology with Swarm Intelligence Feature Optimization Algorithm to Realize High Precision Identification of Aflatoxin-B1 Content in Peanut Oil. *Food Anal. Methods* **2025**, *18*, 1954–1963. [CrossRef]

30. Zhang, X.; Zhou, Y.; Wang, J.; Huang, X.; El-Mesery, H.; Shi, Y.; Zou, Y.; Li, Z.; Li, Y.; Shi, J.; et al. Simple-easy electrochemical sensing mode assisted with integrative carbon-based gel electrolyte for in-situ monitoring of plant hormone indole acetic acid. *Food Chem.* **2025**, *467*, 142342. [CrossRef] [PubMed]
31. Gunathilaka, M.; Bao, S.Y.; Liu, X.X.; Li, Y.; Pan, Y. Antibiotic Pollution of Planktonic Ecosystems: A Review Focused on Community Analysis and the Causal Chain Linking Individual- and Community-Level Responses. *Environ. Sci. Technol.* **2023**, *57*, 1199–1213. [CrossRef] [PubMed]
32. Jayan, H.; Yin, L.; Zhou, R.; Zou, X.; Guo, Z. Future horizons of Raman spectroscopy in food science: Emerging techniques and innovations for enhanced analysis. *Food Chem.* **2025**, *493*, 145777. [CrossRef] [PubMed]
33. Xu, Y.; Kutsanedzie, F.; Hassan, M.; Zhu, J.; Ahmad, W.; Li, H.; Chen, Q. Mesoporous silica supported orderly-spaced gold nanoparticles SERS-based sensor for pesticides detection in food. *Food Chem.* **2020**, *315*, 126300. [CrossRef] [PubMed]
34. Jiao, T.; Hassan, M.; Zhu, J.; Ali, S.; Ahmad, W.; Wang, J.; Lv, C.; Chen, Q.; Li, H. Quantification of deltamethrin residues in wheat by Ag@ZnO NFs-based surface-enhanced Raman spectroscopy coupling chemometric models. *Food Chem.* **2021**, *337*, 127652. [CrossRef] [PubMed]
35. Liu, C.; Xu, D.; Dong, X.; Huang, Q. A review: Research progress of SERS-based sensors for agricultural applications. *Trends Food Sci. Technol.* **2022**, *128*, 90–101. [CrossRef]
36. Zhai, W.L.; You, T.Y.; Ouyang, X.H.; Wang, M. Recent progress in mycotoxins detection based on surface-enhanced Raman spectroscopy. *Compr. Rev. Food Sci. Food Saf.* **2021**, *20*, 1887–1909. [CrossRef] [PubMed]
37. Liu, Z.; Yang, R.; Chen, H.; Zhang, X. Recent Advances in Food Safety: Nanostructure-Sensitized Surface-Enhanced Raman Sensing. *Foods* **2025**, *14*, 1115. [CrossRef] [PubMed]
38. Yu, P.; Shen, C.; Yin, X.; Cheng, J.; Liu, C.; Yu, Z. Au-Ag Bimetallic Nanoparticles for Surface-Enhanced Raman Scattering (SERS) Detection of Food Contaminants: A Review. *Foods* **2025**, *14*, 2109. [CrossRef] [PubMed]
39. Gu, H.; Lv, R.; Huang, X.; Chen, Q.; Dong, Y. Rapid quantitative assessment of lipid oxidation in a rapeseed oil-in-water (o/w) emulsion by three-dimensional fluorescence spectroscopy. *J. Food Compos. Anal.* **2022**, *114*, 104762. [CrossRef]
40. Chang, X.; Huang, X.; Tian, X.; Wang, C.; Aheto, J.; Ernest, B.; Yi, R. Dynamic characteristics of dough during the fermentation process of Chinese steamed bread. *Food Chem.* **2020**, *312*, 126050. [CrossRef] [PubMed]
41. Murugesan, A.; Li, H. Toward Sustainable Food Packaging: Innovations in Biodegradable Materials, Smart Technologies, and AI Integration. *Compr. Rev. Food Sci. Food Saf.* **2026**, *25*, e70397. [CrossRef] [PubMed]
42. Zhao, J.; Fan, S.; Zhang, B.; Wang, A.; Zhang, L.; Zhu, Q. Research Status and Development Trends of Deep Reinforcement Learning in the Intelligent Transformation of Agricultural Machinery. *Agriculture* **2025**, *15*, 1223. [CrossRef]
43. Gan, Z.; Hu, X.; Xu, X.; Zhang, W.; Zou, X.; Shi, J.; Zheng, K.; Arslan, M. A portable test strip based on fluorescent europium-based metal-organic framework for rapid and visual detection of tetracycline in food samples. *Food Chem.* **2021**, *354*, 129501. [CrossRef]
44. Liu, J.; Abbas, I.; Noor, R.S. Development of Deep Learning-Based Variable Rate Agrochemical Spraying System for Targeted Weeds Control in Strawberry Crop. *Agronomy* **2021**, *11*, 1480. [CrossRef]
45. Chen, C.; Zhu, W.; Steibel, J.; Siegford, J.; Han, J.; Norton, T. Classification of drinking and drinker-playing in pigs by a video-based deep learning method. *Biosyst. Eng.* **2020**, *196*, 1–14. [CrossRef]
46. Zhu, H.; Yu, H.; Liang, S.; Wei, Y.; Zhang, L.; Huang, S. Prediction of Apple Quality Indicators Under Different Bagging Treatments Using Hyperspectral Imaging Integrated With a Stacking SDAE-PLSR-RR Deep Learning Model. *J. Food Sci.* **2025**, *90*, e70769. [CrossRef] [PubMed]
47. Bobis, O.; Moise, A.; Ballesteros, I.; Reyes, E.; Durán, S.; Sánchez-Sánchez, J.; Cruz-Quintana, S.; Giampieri, F.; Battino, M.; Alvarez-Suarez, J. Eucalyptus honey: Quality parameters, chemical composition and health-promoting properties. *Food Chem.* **2020**, *325*, 126870. [CrossRef] [PubMed]
48. Wang, J.; Chen, Q.; Belwal, T.; Lin, X.; Luo, Z. Insights into chemometric algorithms for quality attributes and hazards detection in foodstuffs using Raman/surface enhanced Raman spectroscopy. *Compr. Rev. Food Sci. Food Saf.* **2021**, *20*, 2476–2507. [CrossRef] [PubMed]
49. Feng, Z.; Zhu, L.; Zhou, R.; Ntakirutimana, T.; Wei, B.; Wang, D. Transforming Apple Grading: Standards Survey and Deep Learning Insights. *Food Bioprocess Technol.* **2025**, *18*, 5954–5969. [CrossRef]
50. Shang, W.; Wei, G.; Li, H.; Zhao, G.; Wang, D. Advances in High-Resolution Mass Spectrometry-Based Metabolomics: Applications in Food Analysis and Biomarker Discovery. *J. Agric. Food. Chem.* **2025**, *73*, 3305–3325. [CrossRef] [PubMed]
51. Yuan, Y.; Chen, L.; Wu, H.; Li, L. Advanced agricultural disease image recognition technologies: A review. *Inf. Process. Agric.* **2022**, *9*, 48–59. [CrossRef]
52. Wang, Y.; Cai, J.; Lin, H.; Ouyang, Q.; Liu, Z. Deep learning-assisted self-cleaning cellulose colorimetric sensor array for monitoring black tea withering dynamics. *Food Chem.* **2025**, *487*, 144727. [CrossRef] [PubMed]
53. Yan, J.; Wang, C.; Yu, Y.; Wu, L.; Chen, T.; Wang, Z. Physicochemical characteristics and in vitro biological activities of polysaccharides derived from raw garlic (*Allium sativum* L.) bulbs via three-phase partitioning combined with gradient ethanol precipitation method. *Food Chem.* **2021**, *339*, 128081. [CrossRef] [PubMed]

54. Leiva-Valenzuela, G.; Lu, R.; Aguilera, J. Prediction of firmness and soluble solids content of blueberries using hyperspectral reflectance imaging. *J. Food Eng.* **2013**, *115*, 91–98. [CrossRef]
55. Xuan, G.; Gao, C.; Shao, Y. Spectral and image analysis of hyperspectral data for internal and external quality assessment of peach fruit. *Spectrochim. Acta Part A-Mol. Biomol. Spectrosc.* **2022**, *272*, 121016. [CrossRef] [PubMed]
56. Zhang, L.; Sun, J.; Zhou, X.; Nirere, A.; Wu, X.; Dai, R. Classification detection of saccharin jujube based on hyperspectral imaging technology. *J. Food Process. Preserv.* **2020**, *44*, e14591. [CrossRef]
57. Xiao, X.; Fu, L.; Zhang, Z.; Tu, Z.; Shen, N.; Fan, S. Recent Advances in Integrating Machine Learning with Omics Approaches in Food Science and Nutrition Research. *J. Agric. Food. Chem.* **2025**, *73*, 29998–30025. [CrossRef] [PubMed]
58. Tu, H.; Huang, D.; Huang, X.; Aheto, J.; Yi, R.; Yu, W.; Ji, L.; Shuai, N.; Xu, M. Detection of browning of fresh-cut potato chips based on machine vision and electronic nose. *J. Food Process Eng.* **2021**, *44*, e13631. [CrossRef]
59. Li, Z.; An, Y.; Huang, X.; Fang, W.; Guo, Z.; Shi, J.; Zou, X. Integration of multispectral imaging with colorimetric sensor arrays for rapid grading and volatile component prediction of Zhenjiang aromatic vinegar. *Food Chem.* **2025**, *487*, 144454. [CrossRef] [PubMed]
60. Yao, K.; Sun, J.; Tang, N.; Xu, M.; Cao, Y.; Fu, L.; Zhou, X.; Wu, X. Nondestructive detection for Panax notoginseng powder grades based on hyperspectral imaging technology combined with CARS-PCA and MPA-LSSVM. *J. Food Process Eng.* **2021**, *44*, e13718. [CrossRef]
61. Zareef, M.; Arslan, M.; Hassan, M.; Ali, S.; Ouyang, Q.; Li, H.; Wu, X.; Hashim, M.; Javaria, S.; Chen, Q. Application of benchtop NIR spectroscopy coupled with multivariate analysis for rapid prediction of antioxidant properties of walnut (*Juglans regia*). *Food Chem.* **2021**, *359*, 129928. [CrossRef] [PubMed]
62. Duan, N.; Chang, B.; Zhang, H.; Wang, Z.; Wu, S. *Salmonella typhimurium* detection using a surface-enhanced Raman scattering-based aptasensor. *Int. J. Food Microbiol.* **2016**, *218*, 38–43. [CrossRef] [PubMed]
63. Li, H.; Sheng, W.; Adade, S.; Nunekpeku, X.; Chen, Q. Investigation of heat-induced pork batter quality detection and change mechanisms using Raman spectroscopy coupled with deep learning algorithms. *Food Chem.* **2024**, *461*, 140798. [CrossRef] [PubMed]
64. Chen, H.; Geng, D.; Chen, T.; Lu, D.; Chen, B. Second-derivative laser-induced fluorescence spectroscopy combined with chemometrics for authentication of the adulteration of camellia oil. *Cyta-J. Food* **2018**, *16*, 747–754. [CrossRef]
65. Wu, X.; Yuan, Z.; Gao, S.; Zhang, X.; El-Mesery, H.; Lu, W.; Dai, X.; Xu, R. Nanostructure-Engineered Optical and Electrochemical Biosensing Toward Food Safety Assurance. *Foods* **2025**, *14*, 3021. [CrossRef] [PubMed]
66. Kang, W.; Lin, H.; Jiang, H.; Adade, S.; Xue, Z.; Chen, Q. Advanced applications of chemo-responsive dyes based odor imaging technology for fast sensing food quality and safety: A review. *Compr. Rev. Food Sci. Food Saf.* **2021**, *20*, 5145–5172. [CrossRef] [PubMed]
67. Rong, Y.; Hassan, M.; Ouyang, Q.; Chen, Q. Lanthanide ion (Ln^{3+})-based upconversion sensor for quantification of food contaminants: A review. *Compr. Rev. Food Sci. Food Saf.* **2021**, *20*, 3531–3578. [CrossRef] [PubMed]
68. Al-Hooti, H.; Al-Bulushi, I.; Al-Attabi, Z.; Rahman, M.; Al-Subhi, L.; Al-Habsi, N. Efficiency of Electronic Nose in Detecting the Microbial Spoilage of Fresh Sardines (*Sardinella longiceps*). *Foods* **2024**, *13*, 428. [CrossRef] [PubMed]
69. Sun, J.; Zhang, R.; Zhang, Y.; Liang, Q.; Li, G.; Yang, N.; Xu, P.; Guo, J. Classifying fish freshness according to the relationship between EIS parameters and spoilage stages. *J. Food Eng.* **2018**, *219*, 101–110. [CrossRef]
70. Huang, Y.; Li, Z.; Bian, Z.; Jin, H.; Zheng, G.; Hu, D.; Sun, Y.; Fan, C.; Xie, W.; Fang, H. Overview of Deep Learning and Nondestructive Detection Technology for Quality Assessment of Tomatoes. *Foods* **2025**, *14*, 286. [CrossRef] [PubMed]
71. Lv, R.; Huang, X.; Aheto, J.H.; Mu, L.; Tian, X. Analysis of fish spoilage by gas chromatography–mass spectrometry and electronic olfaction bionic system. *J. Food Saf.* **2018**, *38*, e12557. [CrossRef]
72. Huang, B.; Zhang, K.; Kwadzokpui, B.A.; Han, E.; Guan, B.; Lin, H. Real-Time Monitoring and Rapid Determination of Pork Freshness Using a Colorimetric Sensor Array Based on Porphyrin and pH Indicator Ligand Combination. *J. Agric. Food. Chem.* **2025**, *73*, 11327–11339. [CrossRef] [PubMed]
73. Zhou, Y.; Jiao, L.; Wu, J.; Zhang, Y.; Zhu, Q.; Dong, D. Non-destructive and in-situ detection of shrimp freshness using mid-infrared fiber-optic evanescent wave spectroscopy. *Food Chem.* **2023**, *422*, 136189. [CrossRef] [PubMed]
74. Sun, J.; Wang, J.; Lin, W.; Li, B.; Ma, R.; Huang, Y.; Obadi, M. Predict the Gelling Properties of Alkali-Induced Egg White Gel Based on the Freshness of Duck Eggs. *Foods* **2023**, *12*, 4028. [CrossRef] [PubMed]
75. Zulkhairi Amin, F.A.; Shafiq Cheng, M.Z.; Sabri, S.; Ismail, N.; Chan, K.W.; Mohd Esa, N.; Mohd Lila, M.A.; Nur-Fazila, S.H.; Khalifa, S.A.M.; El-Seedi, H.R.; et al. In Vivo Toxicity Assessment of the Probiotic Bacillus amyloliquefaciens HTI-19 Isolated from Stingless Bee (*Heterotrigona itama*) Honey. *Nutrients* **2023**, *15*, 2390. [CrossRef] [PubMed]
76. Liao, J.; Tao, W.Y.; Liang, Y.X.; He, X.Y.; Wang, H.; Zeng, H.Q.; Wang, Z.M.; Luo, X.W.; Sun, J.; Wang, P.; et al. Multi-scale monitoring for hazard level classification of Brown Planthopper damage in rice using hyperspectral technique. *Int. J. Agric. Biol. Eng.* **2024**, *17*, 202–211. [CrossRef]

77. Zhao, J.; Li, H.; Chen, C.; Pang, Y.; Zhu, X. Detection of Water Content in Lettuce Canopies Based on Hyperspectral Imaging Technology under Outdoor Conditions. *Agriculture* **2022**, *12*, 1796. [CrossRef]
78. Liu, C.; Yu, H.; Liu, Y.; Zhang, L.; Li, D.; Zhang, J.; Li, X.; Sui, Y. Prediction of Anthocyanin Content in Purple-Leaf Lettuce Based on Spectral Features and Optimized Extreme Learning Machine Algorithm. *Agronomy* **2024**, *14*, 2915. [CrossRef]
79. Cao, Y.; Sun, J.; Yao, K.; Xu, M.; Tang, N.; Zhou, X. Nondestructive detection of lead content in oilseed rape leaves based on MRF-HHO-SVR and hyperspectral technology. *J. Food Process Eng.* **2021**, *44*, e13793. [CrossRef]
80. Lu, X.Z.; Sun, J.; Mao, H.P.; Wu, X.H.; Gao, H.Y. Quantitative determination of rice starch based on hyperspectral imaging technology. *Int. J. Food Prop.* **2017**, *20*, S1037–S1044. [CrossRef]
81. Bonah, E.; Huang, X.; Aheto, J.; Osae, R. Application of electronic nose as a non-invasive technique for odor fingerprinting and detection of bacterial foodborne pathogens: A review. *J. Food Sci. Technol.-Mysore* **2020**, *57*, 1977–1990. [CrossRef] [PubMed]
82. Jiang, S.Y.; Sun, J.; Xin, Z.; Mao, H.P.; Wu, X.H.; Li, Q.L. Visualizing distribution of pesticide residues in mulberry leaves using NIR hyperspectral imaging. *J. Food Process Eng.* **2017**, *40*, 12510. [CrossRef]
83. Han, F.; Huang, X.; Mahunu, G.K. Exploratory review on safety of edible raw fish per the hazard factors and their detection methods. *Trends Food Sci. Technol.* **2017**, *59*, 37–48. [CrossRef]
84. Cheng, J.; Sun, J.; Shi, L.; Dai, C. An effective method fusing electronic nose and fluorescence hyperspectral imaging for the detection of pork freshness. *Food Biosci.* **2024**, *59*, 103880. [CrossRef]
85. Luo, X.; Sun, C.; He, Y.; Zhu, F.; Li, X. Cross-cultivar prediction of quality indicators of tea based on VIS-NIR hyperspectral imaging. *Ind. Crops Prod.* **2023**, *202*, 117009. [CrossRef]
86. Elsayed, S.; El-Hendawy, S.; Elsherbiny, O.; Okasha, A.M.; Elmetwalli, A.H.; Elwakeel, A.E.; Memon, M.S.; Ibrahim, M.E.M.; Ibrahim, H.H. Estimating Chlorophyll Content, Production, and Quality of Sugar Beet under Various Nitrogen Levels Using Machine Learning Models and Novel Spectral Indices. *Agronomy* **2023**, *13*, 2743. [CrossRef]
87. Khan, J.; Al Jaeed, S.A.; Zhang, Q.; Li, M. Gastronomic tourism and tourist hedonic well-being: A moderated mediation model based on perceived authenticity, emotional connection, and tourist food neophilia. *Int. J. Gastron. Food Sci.* **2025**, *42*, 101294. [CrossRef]
88. Wu, B.; Tang, W.; Zhou, J.; Jia, H.; Shen, H.; Qi, Z. Near-infrared spectroscopy combined with fuzzy fast pseudoinverse linear discriminant analysis to discriminate mee tea grades. *Heliyon* **2024**, *10*, e27732. [CrossRef] [PubMed]
89. Cao, Z.; Wu, X.; Wu, B.; Zhang, Z.; Sun, J. Combining UDT with XGBoost to identify the geographical origin of black beans by near-infrared spectroscopy. *Curr. Res. Food Sci.* **2025**, *11*, 101131. [CrossRef] [PubMed]
90. Johnson, N.; Adade, S.; Ekumah, J.; Kwadzokpui, B.; Yi, X.; Chen, Q. Advances in mechanisms, designs, and applications of colorimetric sensor arrays for food quality control and authenticity verification. *Trends Food Sci. Technol.* **2025**, *160*, 104999. [CrossRef]
91. Li, M.; Cui, J.; Heydari, M.; Song, X.; Yang, X. Blockchain-enabled sustainability and circular economy practices in wine supply chains: A systematic review of digital innovations for traditional fermented beverages. *Syst. Rev.* **2026**, *10*, 1865504. [CrossRef]
92. Lee, J.; Kim, M.; Yoon, J.; Yoo, K.; Byun, S. PA2E: Real-Time Anomaly Detection With Hyperspectral Imaging for Food Safety Inspection. *IEEE Access* **2024**, *12*, 175535–175549. [CrossRef]
93. Tang, C.; He, Y.; Yuan, B.; Li, L.; Luo, L.; You, T. Simultaneous detection of multiple mycotoxins in agricultural products: Recent advances in optical and electrochemical sensing methods. *Compr. Rev. Food Sci. Food Saf.* **2024**, *23*, e70062. [CrossRef]
94. Huang, R.; Zigale, T.T.; Meng, H.; Wang, L.; Dong, Q.; Zeng, K.; Zhang, Z. Cobalt Single-Atom Nanozyme-Enabled Multimodal Lateral Flow Immunoassay for On-Site Ultrasensitive Detection of Tetracycline Residues in Agri-Food Products. *J. Agric. Food. Chem.* **2025**, *73*, 16648–16659. [CrossRef] [PubMed]
95. Wang, Y.; Xu, J.; Qiu, Y.; Li, P.; Liu, B.; Yang, L.; Barnych, B.; Hammock, B.D.; Zhang, C. Highly Specific Monoclonal Antibody and Sensitive Quantum Dot Beads-Based Fluorescence Immunochromatographic Test Strip for Tebuconazole Assay in Agricultural Products. *J. Agric. Food. Chem.* **2019**, *67*, 9096–9103. [CrossRef] [PubMed]
96. Ren, Q.H.; Wu, Y.L.; Zeng, Q.S.; Yang, N. Deep learning based agricultural remote sensing image segmentation: A review. *J. Agric. Eng.* **2026**, *57*, 1954. [CrossRef]
97. Hu, X.; Zhang, M.; Yang, B.; Tao, Y.; Wei, W. Multimodal Sensor Fusion for Non-Destructive Tea Quality Evaluation: Deep Learning-Enabled Methods, Applications, and Challenges. *Foods* **2026**, *15*, 1810. [CrossRef] [PubMed]
98. Xu, L.Z.; Wei, C.C.; Liang, Z.W.; Chai, X.Y.; Li, Y.M.; Liu, Q. Development of rapeseed cleaning loss monitoring system and experiments in a combine harvester. *Biosyst. Eng.* **2019**, *178*, 118–130. [CrossRef]
99. Zhu, J.S.; Cai, J.R.; Sun, B.S.; Xu, Y.J.; Lu, F.; Ma, H.L. Inspection and classification of wheat quality using image processing. *Qual. Assur. Saf. Crops Foods* **2023**, *15*, 43–54. [CrossRef]
100. Huang, X.; Yu, S.; Xu, H.; Aheto, J.H.; Bonah, E.; Ma, M.; Wu, M.; Zhang, X. Rapid and nondestructive detection of freshness quality of postharvest spinaches based on machine vision and electronic nose. *J. Food Saf.* **2019**, *39*, e12708. [CrossRef]
101. Chen, J.; Lian, Y.; Zou, R.; Zhang, S.; Ning, X.B.; Han, M.N. Real-time grain breakage sensing for rice combine harvesters using machine vision technology. *Int. J. Agric. Biol. Eng.* **2020**, *13*, 194–199. [CrossRef]

102. Cheng, J.; Sun, J.; Yao, K.; Xu, M.; Dai, C. Multi-task convolutional neural network for simultaneous monitoring of lipid and protein oxidative damage in frozen-thawed pork using hyperspectral imaging. *Meat Sci.* **2023**, *201*, 109196. [CrossRef] [PubMed]
103. Liu, W.; Hu, J.P.; Liu, J.X.; Yue, R.C.; Zhang, T.F.; Yao, M.J.; Li, J. Method for the navigation line recognition of the ridge without crops via machine vision. *Int. J. Agric. Biol. Eng.* **2024**, *17*, 230–239. [CrossRef]
104. Qiu, D.K.; Guo, T.H.; Yu, S.Q.; Liu, W.; Li, L.; Sun, Z.Z.; Peng, H.H.; Hu, D. Classification of Apple Color and Deformity Using Machine Vision Combined with CNN. *Agriculture* **2024**, *14*, 978. [CrossRef]
105. Memon, M.S.; Chen, S.R.; Shen, B.G.; Liang, R.Z.; Tang, Z.; Wang, S.; Zhou, W.W.; Memon, N. Automatic visual recognition, detection and classification of weeds in cotton fields based on machine vision. *Crop Prot.* **2025**, *187*, 106966. [CrossRef]
106. Zheng, P.; Adade, S.; Rong, Y.; Zhao, S.; Han, Z.; Gong, Y.; Chen, X.; Yu, J.; Huang, C.; Lin, H. Online System for Monitoring the Degree of Fermentation of Oolong Tea Using Integrated Visible-Near-Infrared Spectroscopy and Image-Processing Technologies. *Foods* **2024**, *13*, 1708. [CrossRef] [PubMed]
107. Zhang, Y.A.; Zhao, Z.; Li, X.Y.; Xue, Z.; Jin, M.Z.; Deng, B.Y. Near-Infrared-Based Measurement Method of Mass Flow Rate in Grain Vibration Feeding System. *Agriculture* **2024**, *14*, 1476. [CrossRef]
108. Wang, C.; Luo, X.; Guo, Z.M.; Wang, A.C.; Zhou, R.Y.; Cai, J.R. Influence of the peel on online detecting soluble solids content of pomelo using Vis-NIR spectroscopy coupled with chemometric analysis. *Food Control* **2025**, *167*, 110777. [CrossRef]
109. Zhao, S.; Adade, S.Y.-S.S.; Wang, Z.; Jiao, T.; Ouyang, Q.; Li, H.; Chen, Q. Deep learning and feature reconstruction assisted vis-NIR calibration method for on-line monitoring of key growth indicators during kombucha production. *Food Chem.* **2025**, *463*, 141411. [CrossRef] [PubMed]
110. Cao, Y.; Li, H.; Sun, J.; Zhou, X.; Yao, K.; Nirere, A. Nondestructive determination of the total mold colony count in green tea by hyperspectral imaging technology. *J. Food Process Eng.* **2020**, *43*, 13570. [CrossRef]
111. Tian, X.Y.; Aheto, J.H.; Bai, J.W.; Dai, C.X.; Ren, Y.; Chang, X.H. Quantitative analysis and visualization of moisture and anthocyanins content in purple sweet potato by Vis-NIR hyperspectral imaging. *J. Food Process. Preserv.* **2021**, *45*, e15128. [CrossRef]
112. Yang, S.; Tao, Y.; Maimaiti, X.; Su, W.; Liu, X.; Zhou, J.; Fan, L. Investigation on the exopolysaccharide production from blueberry juice fermented with lactic acid bacteria: Optimization, fermentation characteristics and Vis-NIR spectral model. *Food Chem.* **2024**, *452*, 139589. [CrossRef] [PubMed]
113. Zhou, X.; Liu, Y.; Zhao, C.; Sun, J.; Shi, L.; Cong, S. Nondestructive detection of cadmium content in oilseed rape leaves under different silicon environments using deep transfer learning and Vis-NIR hyperspectral imaging. *Food Chem.* **2025**, *479*, 143799. [CrossRef] [PubMed]
114. Fan, S.X.; Li, J.B.; Xia, Y.; Tian, X.; Guo, Z.M.; Huang, W.Q. Long-term evaluation of soluble solids content of apples with biological variability by using near-infrared spectroscopy and calibration transfer method. *Postharvest Biol. Technol.* **2019**, *151*, 79–87. [CrossRef]
115. Qiao, Y.; Wang, C.; Zhu, W.; Sun, L.; Bai, J.; Zhou, R.; Zhu, Z.; Cai, J. Online assessment of soluble solids content in strawberries using a developed Vis/NIR spectroscopy system with a hanging grasper. *Food Chem.* **2025**, *478*, 143671. [CrossRef] [PubMed]
116. Wei, L.L.; Yang, H.S.; Niu, Y.X.; Zhang, Y.N.; Xu, L.Z.; Chai, X.Y. Wheat biomass, yield, and straw-grain ratio estimation from multi-temporal UAV-based RGB and multispectral images. *Biosyst. Eng.* **2023**, *234*, 187–205. [CrossRef]
117. Zhang, L.Y.; Wang, A.C.; Zhang, H.Y.; Zhu, Q.Z.; Zhang, H.H.; Sun, W.H.; Niu, Y.X. Estimating Leaf Chlorophyll Content of Winter Wheat from UAV Multispectral Images Using Machine Learning Algorithms under Different Species, Growth Stages, and Nitrogen Stress Conditions. *Agriculture* **2024**, *14*, 1064. [CrossRef]
118. Zhang, J.; Dai, L.M.; Huang, Z.W.; Gong, C.D.; Chen, J.J.; Xie, J.S.; Qu, M.Z. Corn Seed Quality Detection Based on Spectroscopy and Its Imaging Technology: A Review. *Agriculture* **2025**, *15*, 390. [CrossRef]
119. Sun, J.; Tang, K.; Wu, X.H.; Dai, C.X.; Chen, Y.; Shen, J.F. Nondestructive identification of green tea varieties based on hyperspectral imaging technology. *J. Food Process Eng.* **2018**, *41*, 12800. [CrossRef]
120. Aheto, J.H.; Huang, X.Y.; Tian, X.Y.; Ren, Y.; Bonah, E.; Alenyorege, E.A.; Lv, R.Q.; Dai, C.X. Combination of spectra and image information of hyperspectral imaging data for fast prediction of lipid oxidation attributes in pork meat. *J. Food Process Eng.* **2019**, *42*, e13225. [CrossRef]
121. Bonah, E.; Huang, X.Y.; Aheto, J.H.; Osae, R. Application of Hyperspectral Imaging as a Nondestructive Technique for Foodborne Pathogen Detection and Characterization. *Foodborne Pathog. Dis.* **2019**, *16*, 712–722. [CrossRef] [PubMed]
122. Aheto, J.H.; Xingyi, H.Y.; Tian, X.Y.; Bonah, E.; Ren, Y.; Alenyorege, E.A.; Dai, C.X. Investigation into crystal size effect on sodium chloride uptake and water activity of pork meat using hyperspectral imaging. *J. Food Process. Preserv.* **2019**, *43*, e14197. [CrossRef]
123. Li, W.; Wu, Y.; Du, L.; Shang, X.; Shi, J. Hyperspectral Imaging for Foreign Matter Detection in Foods: Advances, Challenges, and Future Directions. *Foods* **2025**, *14*, 3026. [CrossRef] [PubMed]
124. Yao, K.S.; Sun, J.; Zhou, X.; Nirere, A.; Tian, Y.; Wu, X.H. Nondestructive detection for egg freshness grade based on hyperspectral imaging technology. *J. Food Process Eng.* **2020**, *43*, 13422. [CrossRef]

125. Aheto, J.H.; Huang, X.Y.; Tian, X.Y.; Lv, R.Q.; Dai, C.X.; Bonah, E.; Chang, X.H. Evaluation of lipid oxidation and volatile compounds of traditional dry-cured pork belly: The hyperspectral imaging and multi-gas-sensory approaches. *J. Food Process Eng.* **2020**, *43*, 13092. [CrossRef]
126. Adade, S.; Lin, H.; Johnson, N.; Nunekpeku, X.; Aheto, J.; Ekumah, J.; Kwadzokpui, B.; Teye, E.; Ahmad, W.; Chen, Q. Advanced food contaminant detection through multi-source data fusion: Strategies, applications, and future perspectives. *Trends Food Sci. Technol.* **2025**, *156*, 104851. [CrossRef]
127. Tian, X.; Aheto, J.; Dai, C.; Ren, Y.; Bai, J. Monitoring microstructural changes and moisture distribution of dry-cured pork: A combined confocal laser scanning microscopy and hyperspectral imaging study. *J. Sci. Food Agric.* **2021**, *101*, 2727–2735. [CrossRef] [PubMed]
128. Sun, J.; Cao, Y.; Zhou, X.; Wu, M.M.; Sun, Y.D.; Hu, Y.H. Detection for lead pollution level of lettuce leaves based on deep belief network combined with hyperspectral image technology. *J. Food Saf.* **2021**, *41*, 12866. [CrossRef]
129. Zhou, X.; Zhao, C.J.; Sun, J.; Cao, Y.; Yao, K.S.; Xu, M. A deep learning method for predicting lead content in oilseed rape leaves using fluorescence hyperspectral imaging. *Food Chem.* **2023**, *409*, 135251. [CrossRef] [PubMed]
130. Ding, Q.; Rehman Sheikh, A.; Pan, W.; Gu, X.; Sun, N.; Su, X.; Luo, L.; Ma, H.; He, R.; Zhang, T. In situ monitoring of grape seed protein hydrolysis by Raman spectroscopy. *J. Food Biochem.* **2021**, *45*, e13646. [CrossRef] [PubMed]
131. Li, H.H.; Zhang, W.; Nunekpeku, X.; Sheng, W.; Chen, Q.S. Investigating the change mechanism and quantitative analysis of minced pork gel quality with different starches using Raman spectroscopy. *Food Hydrocoll.* **2025**, *159*, 110634. [CrossRef]
132. Mei, C.; Lu, S.; Zhou, X.; Meng, F.; Jiang, H. Rapid and Accurate Quantification Detection of BHT in Edible Oils Using Raman Spectroscopy Combined with Chemometric Models. *Foods* **2026**, *15*, 730. [CrossRef] [PubMed]
133. Zhang, X.; Bian, F.; Wang, Y.; Hu, L.; Yang, N.; Mao, H. A Method for Capture and Detection of Crop Airborne Disease Spores Based on Microfluidic Chips and Micro Raman Spectroscopy. *Foods* **2022**, *11*, 3462. [CrossRef] [PubMed]
134. Aheto, J.H.; Huang, X.Y.; Wang, C.Q.; Tian, X.Y.; Yi, R.; Wang, Y.N. Fabrication and evaluation of chitosan modified filter paper for chlorpyrifos detection in wheat by surface-enhanced Raman spectroscopy. *J. Sci. Food Agric.* **2022**, *102*, 7323–7330. [CrossRef] [PubMed]
135. Ma, L.; Yang, X.; Xue, S.; Zhou, R.; Wang, C.; Guo, Z.; Wang, Y.; Cai, J. "Raman plus X" dual-modal spectroscopy technology for food analysis: A review. *Compr. Rev. Food Sci. Food Saf.* **2025**, *24*, e70102. [CrossRef] [PubMed]
136. Deng, J.; Zhao, M.; Jiang, H. Research Progress in the Detection of Mycotoxins in Cereals and Their Products by Vibrational Spectroscopy. *Foods* **2025**, *14*, 2688. [CrossRef] [PubMed]
137. Wang, W.; Zhou, R.; Jayan, H.; Yin, L.; Shao, X.; Zou, X.; Guo, Z. Innovative applications of quantum dots-based surface-enhanced Raman spectroscopy for food safety detection. *Crit. Rev. Food Sci. Nutr.* **2026**, *66*, 791–810. [CrossRef] [PubMed]
138. Ma, L.; Zhou, R.; Yin, L.; Sun, L.; Han, E.; Bai, J.; Cai, J. Simultaneous Detection of Food Contaminants Using Surface-Enhanced Raman Scattering (SERS): A Review. *Foods* **2025**, *14*, 2982. [CrossRef] [PubMed]
139. Li, H.; Hassan, M.; He, Z.; Haruna, S.; Chen, Q.; Ding, Z. A sensitive silver nanoflower-based SERS sensor coupled novel chemometric models for simultaneous detection of chlorpyrifos and carbendazim in food. *Lwt-Food Sci. Technol.* **2022**, *167*, 113804. [CrossRef]
140. Xue, Y.C.; Jiang, H. Monitoring of Chlorpyrifos Residues in Corn Oil Based on Raman Spectral Deep-Learning Model. *Foods* **2023**, *12*, 2402. [CrossRef] [PubMed]
141. Ma, L.; Han, E.; Yin, L.; Xu, Q.; Zou, C.; Bai, J.; Wu, W.; Cai, J. Simultaneous detection of mixed pesticide residues based on portable Raman spectrometer and Au@Ag nanoparticles SERS substrate. *Food Control* **2023**, *153*, 109951. [CrossRef]
142. Liu, R.; Ali, S.; Haruna, S.; Ouyang, Q.; Li, H.; Chen, Q. Development of a fluorescence sensing platform for specific and sensitive detection of pathogenic bacteria in food samples. *Food Control* **2022**, *131*, 108419. [CrossRef]
143. Bi, X.; Li, L.; Luo, L.; Liu, X.; Li, J.; You, T. A ratiometric fluorescence aptasensor based on photoinduced electron transfer from CdTe QDs to WS2 NTs for the sensitive detection of zearalenone in cereal crops. *Food Chem.* **2022**, *385*, 132657. [CrossRef] [PubMed]
144. Li, M.; Qiu, Y.; Liu, G.; Xiao, Y.; Tian, Y.; Fang, S. Plasmonic colorimetry and G-quadruplex fluorescence-based aptasensor: A dual-mode, protein-free and label-free detection for OTA. *Food Chem.* **2024**, *448*, 139115. [CrossRef] [PubMed]
145. Liu, W.; Zhang, R.; Chen, Y.; Gu, W.; Du, H.; Han, Z.; Gao, Z.; Wang, K.; Long, L. Dual-channel fluorescent probe for in-situ differential detection of HClO and H2S in crops and food. *Food Chem.* **2026**, *510*, 148712. [CrossRef] [PubMed]
146. Bilal, M.; Shabbir, M.; Iqbal, W.; Samee-Ullah; Asim, M.; Arslan, M.; Shaukat, F.; Li, Z.; Xia, S.; Xiaobo, Z. Innovative Advances in Colorimetric Sensor Array Technology for Food Safety and Quality Assessment: An Updated Comprehensive Review. *Food Rev. Int.* **2026**, *42*, 1797–1822. [CrossRef]
147. Lu, B.; Sun, J.; Yang, N.; Hang, Y. Fluorescence hyperspectral image technique coupled with HSI method to predict solanine content of potatoes. *J. Food Process. Preserv.* **2019**, *43*, e14198. [CrossRef]
148. Hu, J.; Xie, Y.; Ban, X.; Zhang, L.; Zhou, Z.; Zhang, Z.; Wang, A.; Waine, T. Active Chlorophyll Fluorescence Technologies in Precision Weed Management: Overview and Perspectives. *Agriculture* **2025**, *15*, 1787. [CrossRef]

149. Cheng, J.; Sun, J.; Yao, K.; Xu, M.; Zhou, X. Nondestructive detection and visualization of protein oxidation degree of frozen-thawed pork using fluorescence hyperspectral imaging. *Meat Sci.* **2022**, *194*, 108975. [CrossRef] [PubMed]
150. Chen, X.; Zhao, C.; Zhao, Q.; Yang, Y.; Yang, S.; Zhang, R.; Wang, Y.; Wang, K.; Qian, J.; Long, L. Construction of a Colorimetric and Near-Infrared Ratiometric Fluorescent Sensor and Portable Sensing System for On-Site Quantitative Measurement of Sulfite in Food. *Foods* **2024**, *13*, 1758. [CrossRef] [PubMed]
151. Dai, C.; Huang, X.; Lv, R.; Zhang, Z.; Sun, J.; Aheto, J.H. Analysis of volatile compounds of *Tremella aurantialba* fermentation via electronic nose and HS-SPME-GC-MS. *J. Food Saf.* **2018**, *38*, e12555. [CrossRef]
152. Han, J.; Liang, J.; Yu, X.; Chen, L.; Feng, Y.; Yang, Z.; Mukhtar, A.; Abugri, A.; Zhou, C. Characterization of flavor profiles in chive leaves and stems at different moisture transfer points during combined drying: An integrated approach with e-nose, GC-IMS, GC–MS, and machine learning. *Food Chem.* **2026**, *509*, 148496. [CrossRef] [PubMed]
153. Tian, X.; Dong, H.; Aheto, J.H.; Fang, Q.; Zhang, X.; Dai, C.; Bai, J. Comparative analysis of drying methods on the flavor and quality attributes of ginger (*Zingiber officinale*) using HS-GC-IMS and E-nose. *Food Chem.* **2026**, *513*, 148979. [CrossRef] [PubMed]
154. Zhang, X.; Huang, X.; Dai, C.; Tian, X.; Wang, C.; Ren, Y.; Wang, L.; Yu, S.; Aheto, J.H.; Chang, X. Characterization of volatile flavor profiles and quantitative assessment of key physicochemical indicators for fermented bean curd using GC-IMS, E-nose and multi-channel colorimetric sensor array combined with chemometrics. *Food Biosci.* **2025**, *69*, 106879. [CrossRef]
155. Han, F.K.; Zhang, D.J.; Aheto, J.H.; Feng, F.; Duan, T.F. Integration of a low-cost electronic nose and a voltammetric electronic tongue for red wines identification. *Food Sci. Nutr.* **2020**, *8*, 4330–4339. [CrossRef] [PubMed]
156. Bonah, E.; Huan, X.; Yi, R.; Aheto, J.; Osae, R.; Golly, M. Electronic nose classification and differentiation of bacterial foodborne pathogens based on support vector machine optimized with particle swarm optimization algorithm. *J. Food Process Eng.* **2019**, *42*, 13236. [CrossRef]
157. Han, F.; Huang, X.; Aheto, J.; Zhang, D.; Feng, F. Detection of Beef Adulterated with Pork Using a Low-Cost Electronic Nose Based on Colorimetric Sensors. *Foods* **2020**, *9*, 193. [CrossRef] [PubMed]
158. Yin, L.; Jayan, H.; Cai, J.; El-Seedi, H.; Guo, Z.; Zou, X. Spoilage Monitoring and Early Warning for Apples in Storage Using Gas Sensors and Chemometrics. *Foods* **2023**, *12*, 2968. [CrossRef] [PubMed]
159. Liu, J.; Sun, J.; Wang, Y.; Liu, X.; Zhang, Y.; Fu, H. Non-Destructive Detection of Fruit Quality: Technologies, Applications and Prospects. *Foods* **2025**, *14*, 2137. [CrossRef] [PubMed]
160. Yu, S.; Huang, X.; Wang, L.; Chang, X.; Ren, Y.; Zhang, X.; Wang, Y. Qualitative and quantitative assessment of flavor quality of Chinese soybean paste using multiple sensor technologies combined with chemometrics and a data fusion strategy. *Food Chem.* **2023**, *405*, 134859. [CrossRef] [PubMed]
161. Tian, X.Y.; Aheto, J.H.; Huang, X.Y.; Zheng, K.Y.; Dai, C.X.; Wang, C.Q.; Bai, J.W. An evaluation of biochemical, structural and volatile changes of dry-cured pork using a combined ion mobility spectrometry, hyperspectral and confocal imaging approach. *J. Sci. Food Agric.* **2021**, *101*, 5972–5983. [CrossRef] [PubMed]
162. Zhong, Y.H.; Sun, J.; Yao, K.S.; Cheng, J.H.; Du, X.J. Detection of rice (with husk) moisture content based on hyperspectral imaging technology combined with MSLPP-ESMA-SVR model. *J. Food Saf.* **2024**, *44*, 13112. [CrossRef]
163. Hassan, M.M.; Li, H.H.; Ahmad, W.; Zareef, M.; Wang, J.J.; Xie, S.C.; Wang, P.Y.; Ouyang, Q.; Wang, S.Y.; Chen, Q.S. Au@Ag nanostructure based SERS substrate for simultaneous determination of pesticides residue in tea via solid phase extraction coupled multivariate calibration. *Lwt-Food Sci. Technol.* **2019**, *105*, 290–297. [CrossRef]
164. Niu, Y.X.; Han, W.T.; Zhang, H.H.; Zhang, L.Y.; Chen, H.P. Estimating maize plant height using a crop surface model constructed from UAV RGB images. *Biosyst. Eng.* **2024**, *241*, 56–67. [CrossRef]
165. Shen, T.; Zou, X.; Shi, J.; Li, Z.; Huang, X.; Xu, Y.; Chen, W. Determination Geographical Origin and Flavonoids Content of Goji Berry Using Near-Infrared Spectroscopy and Chemometrics. *Food Anal. Methods* **2016**, *9*, 68–79. [CrossRef]
166. Shi, J.; Hu, X.; Zou, X.; Zhao, J.; Zhang, W.; Holmes, M.; Huang, X.; Zhu, Y.; Li, Z.; Shen, T.; et al. A rapid and nondestructive method to determine the distribution map of protein, carbohydrate and sialic acid on Edible bird's nest by hyper-spectral imaging and chemometrics. *Food Chem.* **2017**, *229*, 235–241. [CrossRef] [PubMed]
167. Li, H.; Wang, Y.; Li, C.; Nunekpeku, X.; Chen, Y.; Zhang, W.; Sheng, W. Non-destructive visualization and prediction of surimi gel quality under atmospheric cold plasma via hyperspectral imaging and deep learning. *Food Control* **2026**, *183*, 111942. [CrossRef]
168. Sun, X.; Zhang, D.; Zhao, L.; Shi, B.; Sun, Y.; Shi, J.; Battino, M.; Wang, G.; Wang, W.; Zou, X. A novel strategy based on dynamic surface-enhanced Raman scattering spectroscopy (D-SERS) for the discrimination and quantification of hydroxyl-sanshools in the pericarps of genus *Zanthoxylum*. *Ind. Crops Prod.* **2022**, *183*, 114940. [CrossRef]
169. Li, H.R.; Pan, T.H.; Li, Y.Q.; Chen, S.; Li, G.Q. Functional principal component analysis for near-infrared spectral data: A case study on Tricholoma matsutakeis. *Int. J. Food Eng.* **2020**, *16*, 20190386. [CrossRef]
170. Jia, W.K.; Zheng, Y.J.; Zhao, D.A.; Yin, X.; Liu, X.Y.; Du, R.C. Preprocessing method of night vision image application in apple harvesting robot. *Int. J. Agric. Biol. Eng.* **2018**, *11*, 158–163. [CrossRef]
171. Dai, C.X.; Huang, X.Y.; Huang, D.M.; Lv, R.Q.; Sun, J.; Zhang, Z.C.; Ma, M.; Aheto, J.H. Detection of submerged fermentation of *Tremella aurantialba* using data fusion of electronic nose and tongue. *J. Food Process Eng.* **2019**, *42*, 13002. [CrossRef]

172. Zhu, W.J.; Li, J.Y.; Li, L.; Wang, A.C.; Wei, X.H.; Mao, H.P. Nondestructive diagnostics of soluble sugar, total nitrogen and their ratio of tomato leaves in greenhouse by polarized spectra-hyperspectral data fusion. *Int. J. Agric. Biol. Eng.* **2020**, *13*, 189–197. [CrossRef]
173. Ren, Y.; Huang, X.; Aheto, J.H.; Wang, C.; Ernest, B.; Tian, X.; He, P.; Chang, X.; Wang, C. Application of volatile and spectral profiling together with multimode data fusion strategy for the discrimination of preserved eggs. *Food Chem.* **2021**, *343*, 128515. [CrossRef] [PubMed]
174. Awais, M.; Li, W.; Hussain, S.; Cheema, M.J.M.; Li, W.G.; Song, R.; Liu, C.C. Comparative Evaluation of Land Surface Temperature Images from Unmanned Aerial Vehicle and Satellite Observation for Agricultural Areas Using In Situ Data. *Agriculture* **2022**, *12*, 184. [CrossRef]
175. Yolandani; Liu, D.; Raynaldo, F.A.; Dabbour, M.; Zhang, X.; Chen, Z.; Ding, Q.; Luo, L.; Ma, H. Comparison of prediction models for soy protein isolate hydrolysates bitterness built using sensory, spectrofluorometric and chromatographic data from varying enzymes and degree of hydrolysis. *Food Chem.* **2024**, *442*, 138428. [CrossRef] [PubMed]
176. Huang, B. Process identification based on last principal component analysis. *J. Process Control* **2001**, *11*, 19–33. [CrossRef]
177. Hellton, K.; Thoresen, M. When and Why are Principal Component Scores a Good Tool for Visualizing High-dimensional Data? *Scand. J. Stat.* **2017**, *44*, 581–597. [CrossRef]
178. Zhang, B.; Bai, T.C.; Wu, G.; Wang, H.W.; Zhu, Q.Z.; Zhang, G.Q.; Meng, Z.J.; Wen, C.K. Fatigue Analysis of Shovel Body Based on Tractor Subsoiling Operation Measured Data. *Agriculture* **2024**, *14*, 1604. [CrossRef]
179. Sun, J.; He, X.; Ge, X.; Wu, X.; Shen, J.; Song, Y. Detection of Key Organs in Tomato Based on Deep Migration Learning in a Complex Background. *Agriculture* **2018**, *8*, 196. [CrossRef]
180. Peng, Y.; Wang, A.; Liu, J.; Faheem, M. A Comparative Study of Semantic Segmentation Models for Identification of Grape with Different Varieties. *Agriculture* **2021**, *11*, 997. [CrossRef]
181. Yang, N.; Chang, K.P.; Dong, S.Z.; Tang, J.; Wang, A.Y.; Huang, R.B.; Jia, Y.W. Rapid image detection and recognition of rice false smut based on mobile smart devices with anti-light features from cloud database. *Biosyst. Eng.* **2022**, *218*, 229–244. [CrossRef]
182. Wang, Z.; Wang, Q.; Li, J.; Huang, W. Non-destructive detection of soluble solids content in Shawo radish with spatial spectra extraction method based on the full transmission near-infrared spectroscopy. *J. Food Compos. Anal.* **2025**, *148*, 108364. [CrossRef]
183. Li, H.H.; Li, C.H.; Nunekpeku, X.; Sheng, W.; Zhang, W.; Adade, S. Deep learning-enhanced multi-modal data fusion for predicting gel strength and water holding capacity in ultrasonically processed pork. *Food Control* **2026**, *180*, 111680. [CrossRef]
184. Wang, Q.; Zhao, M.; Zabed, H.M.; Tang, X.R.; Chen, J.J.; Wang, J.Y.; Li, H.Y.; Qi, X.H. Data-Driven Mining of a Thermostable Lipase with Molecular Insights into Mechanisms of Its Substrate Specificity. *J. Agric. Food. Chem.* **2025**, *73*, 17739–17749. [CrossRef] [PubMed]
185. Wang, Q.; Zabed, H.M.; Zhao, M.; Qi, X.H. A Deeper Insight into the Thermostability of a Novel Laccase Designed by Data-Driven Mining and Rational Engineering. *J. Agric. Food. Chem.* **2025**, *73*, 23498–23509. [CrossRef] [PubMed]
186. Luo, W.; Li, Q.C.; Zhang, H.L.; Diao, Z.H.; Guo, Z.M.; Cai, Z.L.; Zhang, Y.Z.; Li, J.B. Detection of early decay in dekopon fruit based on structured-illumination reflectance imaging combined with a comparison between traditional machine learning and deep learning models. *Postharvest Biol. Technol.* **2026**, *233*, 114044. [CrossRef]
187. Zhang, Z.; Lu, Y.Z.; Yang, M.Y.; Wang, G.Q.; Zhao, Y.Q.; Hu, Y.G. Optimal training strategy for high-performance detection model of multi-cultivar tea shoots based on deep learning methods. *Sci. Hortic.* **2024**, *328*, 112949. [CrossRef]
188. Zheng, K.; Yang, S.; Wang, Z.C.; Fu, H.; Wang, X.; Zou, W.; Zhai, C.Y.; Chen, L.P. Real-Time Detection and Validation of a Target-Oriented Model for Spindle-Shaped Tree Trunks Leveraging Deep Learning. *Agronomy* **2026**, *16*, 210. [CrossRef]
189. Chen, L.; Wu, Y.; Yang, N.; Sun, Z.B. Advances in Hyperspectral and Diffraction Imaging for Agricultural Applications. *Agriculture* **2025**, *15*, 1775. [CrossRef]
190. Liu, X.; Sun, Z.; Zuo, M.; Zou, X.; Wang, T.; Li, J. Quantitative detection of restructured steak adulteration based on hyperspectral technology combined with a wavelength selection algorithm cascade strategy. *Food Sci. Technol. Res.* **2021**, *27*, 859–869. [CrossRef]
191. Ahmed, S.; Qiu, B.J.; Kong, C.W.; Xin, H.; Ahmad, F.; Lin, J.L. A Data-Driven Dynamic Obstacle Avoidance Method for Liquid-Carrying Plant Protection UAVs. *Agronomy* **2022**, *12*, 873. [CrossRef]
192. Cai, L.T.; Zhang, Y.Z.; Cai, Z.L.; Shi, R.Y.; Li, S.; Li, J.B. Detection of soluble solids content in tomatoes using full transmission Vis-NIR spectroscopy and combinatorial algorithms. *Front. Plant Sci.* **2024**, *15*, 1500819. [CrossRef] [PubMed]
193. Duras, T. The fixed effects PCA model in a common principal component environment. *Commun. Stat.-Theory Methods* **2022**, *51*, 1653–1673. [CrossRef]
194. Sarabia, L.A.; Ortiz, M.C.; Sánchez, M.S.; Herrero, A. Partial least squares fine-tuning by a bootstrap estimated signal-noise relation to weight the loadings. *Chemom. Intell. Lab. Syst.* **2003**, *68*, 83–96. [CrossRef]
195. Aminu, M.; Ahmad, N.A. Locality preserving partial least squares discriminant analysis for face recognition. *J. King Saud Univ. Comput. Inf. Sci.* **2022**, *34*, 153–164. [CrossRef]
196. Yao, K.; Sun, J.; Chen, C.; Xu, M.; Zhou, X.; Cao, Y.; Tian, Y. Non-destructive detection of egg qualities based on hyperspectral imaging. *J. Food Eng.* **2022**, *325*, 111024. [CrossRef]

197. Wen, C.T.; Zhang, J.X.; Duan, Y.Q.; Zhang, H.H.; Ma, H.L. A Mini-Review on Brewer's Spent Grain Protein: Isolation, Physicochemical Properties, Application of Protein, and Functional Properties of Hydrolysates. *J. Food Sci.* **2019**, *84*, 3330–3340. [CrossRef] [PubMed]
198. Akgül, A.; Akgül, E.K.; Korhan, S. New reproducing kernel functions in the reproducing kernel Sobolev spaces. *Aims Math.* **2020**, *5*, 482–496. [CrossRef]
199. Zhang, X.D.; Li, T.Z.; Guo, C.D.; Zhang, D.S.; Zhang, Y.X. Utilizing Multi-View Morphological, Color-Textural and Multispectral Features for Interpretable Estimation of Lettuce Fresh Weight Using Machine Learning. *Horticulturae* **2026**, *12*, 688. [CrossRef]
200. Zhu, W.; Ma, L.; Shi, Z.; Qiao, Y.; Li, Q.; Pan, B.; Feng, Z.; Yang, X.; Cai, J.; Bai, J.; et al. Early-stage fertilised egg viability detection based on machine vision. *Br. Poult. Sci.* **2025**, *66*, 613–624. [CrossRef] [PubMed]
201. Li, H.H.; Nunekpeku, X.; Zhang, W.; Adade, S.; Ahmad, W.; Sheng, W.; Chen, Q.S. Quantitative prediction of minced chicken gel strength under ultrasonic treatment by NIR spectroscopy coupled with nonlinear chemometric tools evaluated using APaRPs. *Food Chem.* **2025**, *463*, 141373. [CrossRef] [PubMed]
202. Sun, J.; Nirere, A.; Dusabe, K.D.; Zhong, Y.H.; Adrien, G. Rapid and nondestructive watermelon (*Citrullus lanatus*) seed viability detection based on visible near-infrared hyperspectral imaging technology and machine learning algorithms. *J. Food Sci.* **2024**, *89*, 4403–4418. [CrossRef] [PubMed]
203. Zhu, X.; Wu, X.H.; Shen, J.F.; Sun, J.; Wu, B. Near-infrared spectroscopy coupled with machine learning algorithms based on L1-norm and L21-norm to identify the geographical origins of Chinese wolfberry. *Food Chem.* **2025**, *493*, 145863. [CrossRef] [PubMed]
204. Chang, X.H.; Huang, X.Y.; Xu, W.D.; Tian, X.Y.; Wang, C.Q.; Wang, L.; Yu, S.S. Monitoring of dough fermentation during Chinese steamed bread processing by near-infrared spectroscopy combined with spectra selection and supervised learning algorithm. *J. Food Process Eng.* **2021**, *44*, e13783. [CrossRef]
205. Xu, M.; Sun, J.; Cheng, J.H.; Yao, K.N.; Wu, X.H.; Zhou, X. Non-destructive prediction of total soluble solids and titratable acidity in Kyoho grape using hyperspectral imaging and deep learning algorithm. *Int. J. Food Sci. Technol.* **2023**, *58*, 9–21. [CrossRef]
206. Elbeltagi, A.; Srivastava, A.; Deng, J.S.; Li, Z.B.; Raza, A.; Khadke, L.; Yu, Z.L.; El-Rawy, M. Forecasting vapor pressure deficit for agricultural water management using machine learning in semi-arid environments. *Agric. Water Manag.* **2023**, *283*, 108302. [CrossRef]
207. Xie, C.Q.; He, Y. External characteristic determination of eggs and cracked eggs identification using spectral signature. *Sci. Rep.* **2016**, *6*, 21130. [CrossRef] [PubMed]
208. Ouyang, Q.; Fan, Z.; Chang, H.; Shoaib, M.; Chen, Q. Analyzing TVB-N in snakehead by Bayesian-optimized 1D-CNN using molecular vibrational spectroscopic techniques: Near-infrared and Raman spectroscopy. *Food Chem.* **2025**, *464*, 141701. [CrossRef] [PubMed]
209. Jiang, Q.; Liu, M.; Wang, Z.; Zhang, R.; Wang, Y.; Guo, F.; Sun, Q.; Ren, C. Low-field NMR-based deep learning for non-destructive quality assessment of frozen model foods. *Food Chem.* **2025**, *489*, 145181. [CrossRef] [PubMed]
210. Lin, H.; Pan, T.H.; Li, Y.Q.; Chen, S.; Li, G.Q. Development of analytical method associating near-infrared spectroscopy with one-dimensional convolution neural network: A case study. *J. Food Meas. Charact.* **2021**, *15*, 2963–2973. [CrossRef]
211. Zhao, S.Y.; Peng, Y.; Liu, J.Z.; Wu, S. Tomato Leaf Disease Diagnosis Based on Improved Convolution Neural Network by Attention Module. *Agriculture* **2021**, *11*, 651. [CrossRef]
212. Wang, B.; Deng, J.; Jiang, H. Markov Transition Field Combined with Convolutional Neural Network Improved the Predictive Performance of Near-Infrared Spectroscopy Models for Determination of Aflatoxin B_1 in Maize. *Foods* **2022**, *11*, 2210. [CrossRef] [PubMed]
213. Huang, Y.; Pan, Y.; Liu, C.; Zhou, L.; Tang, L.; Wei, H.; Fan, K.; Wang, A.; Tang, Y. Rapid and Non-Destructive Geographical Origin Identification of Chuanxiong Slices Using Near-Infrared Spectroscopy and Convolutional Neural Networks. *Agriculture* **2024**, *14*, 1281. [CrossRef]
214. Pan, Y.Z.; Jin, H.; Gao, J.C.; Rauf, H.T. Identification of Buffalo Breeds Using Self-Activated-Based Improved Convolutional Neural Networks. *Agriculture* **2022**, *12*, 1386. [CrossRef]
215. Peng, Y.; Sun, J.; Wu, Z.; Shi, L.; Ji, X.; Jia, Y.; Xie, Y. Apple maturity quantification based on fine-grained coloration analysis using deep learning and computer vision. *J. Food Meas. Charact.* **2025**, *19*, 9637–9653. [CrossRef]
216. Sun, C.; Zhang, L.; Zhai, L.; Shen, T.; Cai, J.; Zou, X.; Guo, Z. Automatic early bruise detection in strawberry fruit by hyperspectral imaging and deep learning techniques. *Postharvest Biol. Technol.* **2026**, *232*, 113966. [CrossRef]
217. Yang, C.; Guo, Z.; Barbin, D.; Dai, Z.; Watson, N.; Povey, M.; Zou, X. Hyperspectral Imaging and Deep Learning for Quality and Safety Inspection of Fruits and Vegetables: A Review. *J. Agric. Food. Chem.* **2025**, *73*, 10019–10035. [CrossRef] [PubMed]
218. Cheng, J.H.; Sun, J.; Yao, K.S.; Dai, C.X. Generalized and hetero two-dimensional correlation analysis of hyperspectral imaging combined with three-dimensional convolutional neural network for evaluating lipid oxidation in pork. *Food Control* **2023**, *153*, 109940. [CrossRef]

219. Xi, Q.; Chen, Q.; Ahmad, W.; Pan, J.; Zhao, S.; Xia, Y.; Ouyang, Q.; Chen, Q. Quantitative analysis and visualization of chemical compositions during shrimp flesh deterioration using hyperspectral imaging: A comparative study of machine learning and deep learning models. *Food Chem.* **2025**, *481*, 143997. [CrossRef] [PubMed]
220. Fan, S.; Liu, Q.; Ma, D.; Zhu, Y.; Zhang, L.; Wang, A.; Zhu, Q. Maize Seed Variety Classification Based on Hyperspectral Imaging and a CNN-LSTM Learning Framework. *Agronomy* **2025**, *15*, 1585. [CrossRef]
221. Elsherbiny, O.; Gao, J.; Guo, Y.; Tunio, M.; Mosha, A. Fusion of the deep networks for rapid detection of branch-infected aeroponically cultivated mulberries using multimodal traits. *Int. J. Agric. Biol. Eng.* **2025**, *18*, 75–88. [CrossRef]
222. Cong, S.; Sun, J.; Shi, L.; Dai, C.; Wu, X.; Zhang, B.; Yao, K.; Ge, X. Nondestructive assessment of refrigerated quality attributes of kiwifruit via hyperspectral imaging coupled with a point-to-interval prediction model. *Food Chem.* **2026**, *499*, 147323. [CrossRef] [PubMed]
223. Ji, W.; Zhai, K.L.; Xu, B.; Wu, J.W. Green Apple Detection Method Based on Multidimensional Feature Extraction Network Model and Transformer Module. *J. Food Prot.* **2025**, *88*, 100397. [CrossRef] [PubMed]
224. Sun, C.C.; Li, C.H.; Lin, X.; Zheng, T.J.; Meng, F.R.; Rui, X.B.; Wang, Z.X. Attention-based graph neural networks: A survey. *Artif. Intell. Rev.* **2023**, *56*, 2263–2310. [CrossRef]
225. Kang, H.; Zhang, X.W.; Han, W.P.; Zhou, M.L. Dark knowledge association guided hashing for unsupervised cross-modal retrieval. *Multimed. Syst.* **2024**, *30*, 375. [CrossRef]
226. Xue, D.Y.; Gong, Y.K.; Yang, Z.Y.; Chuai, G.H.; Qu, S.; Shen, A.Z.; Yu, J.; Liu, Q. Advances and challenges in deep generative models for de novo molecule generation. *Wiley Interdiscip. Rev.-Comput. Mol. Sci.* **2019**, *9*, e1395. [CrossRef]
227. Sixou, B.; Mory, C. Kullback-leibler residual and regularization for inverse problems with noisy data and noisy operator. *Inverse Probl. Imaging* **2019**, *13*, 1113–1137. [CrossRef]
228. Zhai, Z.H. Auto-encoder generative adversarial networks. *J. Intell. Fuzzy Syst.* **2018**, *35*, 3043–3049. [CrossRef]
229. Liu, K.L.; Qiu, G.P.; Tang, W.M.; Zhou, F. Spectral regularization for combating mode collapse in GANs. *Image Vis. Comput.* **2020**, *104*, 104005. [CrossRef]
230. Tahir, H.; Zou, X.; Huang, X.; Shi, J.; Mariod, A. Discrimination of honeys using colorimetric sensor arrays, sensory analysis and gas chromatography techniques. *Food Chem.* **2016**, *206*, 37–43. [CrossRef] [PubMed]
231. Li, Z.; Fang, W.; Wang, S.; Shi, J.; Zou, X.; Huang, X. Identification of characteristic volatiles of Zhenjiang aromatic vinegar using HS-SPME-GC/MS coupled with multivariate analysis. *Flavour Fragr. J.* **2024**, *39*, 271–281. [CrossRef]
232. Shen, G.; Kang, X.; Su, J.; Qiu, J.; Liu, X.; Xu, J.; Shi, J.; Mohamed, S. Rapid detection of fumonisin B_1 and B_2 in ground corn samples using smartphone-controlled portable near-infrared spectrometry and chemometrics. *Food Chem.* **2022**, *384*, 132487. [CrossRef] [PubMed]
233. Gu, H.; Liu, K.; Huang, X.; Chen, Q.; Sun, Y.; Tan, C. Feasibility study for the analysis of coconut water using fluorescence spectroscopy coupled with PARAFAC and SVM methods. *Br. Food J.* **2020**, *122*, 3203–3212. [CrossRef]
234. Meng, F.; Zhu, J.; Deng, J.; Wu, T.; Qi, A.; Zhu, W.; Jiang, H. Qualitative and quantitative pesticide residue analysis in *Allium tuberosum* using an electronic nose with multivariate analysis. *Food Chem.* **2025**, *492*, 145661. [CrossRef] [PubMed]
235. Guo, Z.; Zou, Y.; Sun, C.; Jayan, H.; Jiang, S.; El-Seedi, H.; Zou, X. Nondestructive determination of edible quality and watercore degree of apples by portable Vis/NIR transmittance system combined with CARS-CNN. *J. Food Meas. Charact.* **2024**, *18*, 4058–4073. [CrossRef]
236. Wang, C.; Qiao, Y.; Li, X.; Sun, L.; Qiu, G.; Zhou, R.; Guo, Z.; Cai, J. Improving SSC detection accuracy of hanging-transported strawberries through different correction methods and 1D-CNN. *Food Control* **2026**, *181*, 111782. [CrossRef]
237. Daniya, T.; Vigneshwari, S. Deep Neural Network for Disease Detection in Rice Plant Using the Texture and Deep Features. *Comput. J.* **2022**, *65*, 1812–1825. [CrossRef]
238. Mjahad, A.; Rosado-Muñoz, A. Automated Vegetable Classification Using Hybrid CNN and Vision Transformer Models for Food Quality Assessment. *Electronics* **2026**, *15*, 1123. [CrossRef]
239. Yuan, Z.C.; Huang, X.W.; Zhang, X.N.; Gao, S.J.; Chen, H.L.; Li, Z.H.; El-Mesery, H.S.; Shi, J.Y.; Zou, X.B. Unveiling rheological behavior of hydrogels toward Magic 3D printing patterns. *Food Hydrocoll.* **2025**, *168*, 111505. [CrossRef]
240. Huang, X.; Lv, R.; Wang, S.; Aheto, J.; Dai, C. Integration of computer vision and colorimetric sensor array for nondestructive detection of mango quality. *J. Food Process Eng.* **2018**, *41*, 12873. [CrossRef]
241. Li, H.; Kutsanedzie, F.; Zhao, J.; Chen, Q. Quantifying Total Viable Count in Pork Meat Using Combined Hyperspectral Imaging and Artificial Olfaction Techniques. *Food Anal. Methods* **2016**, *9*, 3015–3024. [CrossRef]
242. Zhang, Y.; Zhang, B.; Shen, C.; Liu, H.; Huang, J.; Tian, K.; Tang, Z. Review of the field environmental sensing methods based on multi-sensor information fusion technology. *Int. J. Agric. Biol. Eng.* **2024**, *17*, 1–13. [CrossRef]
243. Liu, H.L.; Zhan, B.S.; Fang, R.T.; Zhang, Y.; Ma, Y.J.; Shen, Z.; Mao, Q.R. Recent advances in pest and disease recognition: A comprehensive review. *J. Agric. Eng.* **2025**, *56*, 1776. [CrossRef]
244. Gu, Y.B.; Yang, M.L.; Shi, Z.G.; Wu, Z.L. The Applications of Decision-Level Data Fusion Techniques in the Field of Multiuser Detection for DS-UWB Systems. *Sensors* **2015**, *15*, 24771–24790. [CrossRef] [PubMed]

245. Sun, J.; Zhang, L.; Zhou, X.; Yao, K.; Tian, Y.; Nirere, A. A method of information fusion for identification of rice seed varieties based on hyperspectral imaging technology. *J. Food Process Eng.* **2021**, *44*, e13797. [CrossRef]
246. Zhu, J.; Meng, F.; Feng, Z.; Wu, T.; Wei, M.; Jiang, H. Procymidone residue detection in *Allium tuberosum* using feature-level data fusion of colorimetric sensor arrays and electronic nose sensor arrays: Comparison of heterogeneous data fusion methods. *Food Chem.* **2026**, *501*, 147544. [CrossRef] [PubMed]
247. Shi, L.; Sun, J.; Cong, S.; Zhang, B.; Zhou, X.; Wu, X. Nondestructive detection of trace cadmium in lettuce leaves using deep fusion of fluorescence hyperspectral imaging and near-infrared spectroscopy. *J. Food Compos. Anal.* **2025**, *147*, 108038. [CrossRef]
248. Zhang, Y.; Chen, W. Decision-level information fusion powered human pose estimation. *Appl. Intell.* **2023**, *53*, 2161–2172. [CrossRef]
249. Xu, X.; Chen, J.; Fu, C.; Lyu, Z. Hypercomplex Neural Network and Cross-Modal Attention for Multi-Modal Emotion Recognition Using Physiological Signals. *IEEE Trans. Affect. Comput.* **2025**, *16*, 3523–3536. [CrossRef]
250. Chen, J.; Song, S.; Tan, Y.; Xia, H. TEMSA: Text enhanced modal representation learning for multimodal sentiment. *Comput. Vis. Image Underst.* **2025**, *258*, 104391. [CrossRef]
251. Dai, Q.; Cheng, J.; Sun, D.; Zhu, Z.; Pu, H. Prediction of total volatile basic nitrogen contents using wavelet features from visible/near-infrared hyperspectral images of prawn (*Metapenaeus ensis*). *Food Chem.* **2016**, *197*, 257–265. [CrossRef] [PubMed]
252. Hughes, J.; Haran, M. Dimension reduction and alleviation of confounding for spatial generalized linear mixed models. *J. R. Stat. Soc. Ser. B-Stat. Methodol.* **2013**, *75*, 139–159. [CrossRef]
253. Yao, K.; Xu, Y.; Sun, J.; Zhou, B.; Zhang, B.; Du, X.; Zhang, Y. Simultaneous detection and visualization of lipid and protein oxidation in frozen-thawed chicken meat using hyperspectral imaging. *Food Res. Int.* **2026**, *229*, 118463. [CrossRef] [PubMed]
254. Jiang, H.; He, Y.; Chen, Q. Qualitative identification of the edible oil storage period using a homemade portable electronic nose combined with multivariate analysis. *J. Sci. Food Agric.* **2021**, *101*, 3448–3456. [CrossRef] [PubMed]
255. Raza, A.; Saber, K.; Hu, Y.; Ray, R.; Kaya, Y.; Dehghanisanij, H.; Kisi, O.; Elbeltagi, A. Modelling reference evapotranspiration using principal component analysis and machine learning methods under different climatic environments. *Irrig. Drain.* **2023**, *72*, 945–970. [CrossRef]
256. Yu, K.; Zhong, M.; Zhu, W.; Rashid, A.; Han, R.; Virk, M.; Duan, K.; Zhao, Y.; Ren, X. Advances in Computer Vision and Spectroscopy Techniques for Non-Destructive Quality Assessment of *Citrus* Fruits: A Comprehensive Review. *Foods* **2025**, *14*, 386. [CrossRef] [PubMed]
257. Dai, C.; Sun, J.; Huang, X.; Zhang, X.; Tian, X.; Wang, W.; Sun, J.; Luan, Y. Application of Hyperspectral Imaging as a Nondestructive Technology for Identifying Tomato Maturity and Quantitatively Predicting Lycopene Content. *Foods* **2023**, *12*, 2957. [CrossRef] [PubMed]
258. Lv, G.; Zhang, W.; Liu, X.; Zhang, J.; Liu, F.; Mao, H.; Sun, W.; Han, Q.; Song, J. Feasibility of Nondestructive Soluble Sugar Monitoring in Tomato: Quantified and Sorted through ATR-FTIR Coupled with Chemometrics. *Agronomy* **2024**, *14*, 2392. [CrossRef]
259. Guo, Z.; Wang, M.; Barimah, A.; Chen, Q.; Li, H.; Shi, J.; El-Seedi, H.; Zou, X. Label-free surface enhanced Raman scattering spectroscopy for discrimination and detection of dominant apple spoilage fungus. *Int. J. Food Microbiol.* **2021**, *338*, 108990. [CrossRef] [PubMed]
260. Nie, R.; Huang, X.; Tian, X.; Yu, S.; Dai, C.; Zhang, X.; Fang, Q. Non-Destructive Detection of Pomegranate Blackheart Disease via Near-Infrared Spectroscopy and Soft X-ray Imaging Systems. *Foods* **2025**, *14*, 2454. [CrossRef] [PubMed]
261. Guo, Z.; Wang, M.; Shujat, A.; Wu, J.; El-Seedi, H.; Shi, J.; Ouyang, Q.; Chen, Q.; Zou, X. Nondestructive monitoring storage quality of apples at different temperatures by near-infrared transmittance spectroscopy. *Food Sci. Nutr.* **2020**, *8*, 3793–3805. [CrossRef] [PubMed]
262. Shi, L.; Sun, J.; Zhang, B.; Wu, Z.; Jia, Y.; Yao, K.; Zhou, X. Simultaneous detection for storage condition and storage time of yellow peach under different storage conditions using hyperspectral imaging with multi-target characteristic selection and multi-task model. *J. Food Compos. Anal.* **2024**, *135*, 106647. [CrossRef]
263. Sun, J.; Lu, X.; Mao, H.; Jin, X.; Wu, X. A Method for rapid identification of rice origin by hyperspectral imaging technology. *J. Food Process Eng.* **2017**, *40*, 12297. [CrossRef]
264. Arslan, M.; Zareef, M.; Afzal, M.; Tahir, H.; Shi, J.; Muhammad, A.; Rakha, A.; Xiaobo, Z. A smart olfactory visualization system based on colorimetric sensor array and chemometrics for the identification of rice adulteration. *Food Chem.* **2025**, *492*, 145581. [CrossRef] [PubMed]
265. Liang, Y.; Lin, H.; Kang, W.; Shao, X.; Cai, J.; Li, H.; Chen, Q. Application of colorimetric sensor array coupled with machine-learning approaches for the discrimination of grains based on freshness. *J. Sci. Food Agric.* **2023**, *103*, 6790–6799. [CrossRef] [PubMed]
266. Lin, H.; Chen, Z.; Adade, S.; Yang, W.; Chen, Q. Detection of Maize Mold Based on a Nanocomposite Colorimetric Sensor Array under Different Substrates. *J. Agric. Food. Chem.* **2024**, *72*, 11164–11173. [CrossRef] [PubMed]

267. Lin, H.; Yan, S.; Song, B.; Wang, Z.; Sun, L. Discrimination of aged rice using colorimetric sensor array combined with volatile organic compounds. *J. Food Process Eng.* **2019**, *42*, 13037. [CrossRef]
268. Chen, Z.; Lin, H.; Wang, F.; Adade, S.; Peng, T.; Chen, Q. Discrimination of toxigenic and non-toxigenic *Aspergillus flavus* in wheat based on nanocomposite colorimetric sensor array. *Food Chem.* **2024**, *430*, 137048. [CrossRef] [PubMed]
269. Sun, J.; Yang, F.; Cheng, J.; Wang, S.; Fu, L. Nondestructive identification of soybean protein in minced chicken meat based on hyperspectral imaging and VGG16-SVM. *J. Food Compos. Anal.* **2024**, *125*, 105713. [CrossRef]
270. Luo, W.; Deng, J.; Li, C.; Jiang, H. Quantitative Analysis of Peanut Skin Adulterants by Fourier Transform Near-Infrared Spectroscopy Combined with Chemometrics. *Foods* **2025**, *14*, 466. [CrossRef] [PubMed]
271. Zhang, F.; Cui, X.; Zhang, C.; Cao, W.; Wang, X.; Fu, S.; Teng, S. Rapid non-destructive identification of selenium-enriched millet based on hyperspectral imaging technology. *Czech. J. Food Sci.* **2022**, *40*, 445–455. [CrossRef]
272. Lin, H.; Jiang, H.; Lin, J.; Chen, Q.; Ali, S.; Teng, S.; Zuo, M. Rice Freshness Identification Based on Visible Near-Infrared Spectroscopy and Colorimetric Sensor Array. *Food Anal. Methods* **2021**, *14*, 1305–1314. [CrossRef]
273. Jiao, X.; Huang, X.; Yu, S.; Wang, L.; Wang, Y.; Zhang, X.; Ren, Y. A novel composite colorimetric sensor array for quality characterization of shrimp paste based on indicator displacement assay and etching of silver nanoprisms. *J. Food Process Eng.* **2023**, *46*, 14195. [CrossRef]
274. Zhang, Y.; Zareef, M.; Rong, Y.; Lin, H.; Chen, Q.; Ouyang, Q. Application of colorimetric sensor array coupled with chemometric methods for monitoring the freshness of snakehead fillets. *Food Chem.* **2024**, *439*, 138172. [CrossRef] [PubMed]
275. Bonah, E.; Huang, X.; Yang, H.; Aheto, J.; Ren, Y.; Yu, S.; Tu, H. Detection of *Salmonella typhimurium* contamination levels in fresh pork samples using electronic nose smellprints in tandem with support vector machine regression and metaheuristic optimization algorithms. *J. Food Sci. Technol.-Mysore* **2021**, *58*, 3861–3870. [CrossRef] [PubMed]
276. Li, H.; Sun, X.; Pan, W.; Kutsanedzie, F.; Zhao, J.; Chen, Q. Feasibility study on nondestructively sensing meat's freshness using light scattering imaging technique. *Meat Sci.* **2016**, *119*, 102–109. [CrossRef] [PubMed]
277. Li, H.; Sheng, W.; Nunekpeku, X.; Hu, Y.; Chen, Q. Prediction of thermal processing effects on gel strength and water holding capacity in pork batter gels: An integrated approach using Raman spectroscopy and chemometric techniques. *Food Control* **2025**, *175*, 111298. [CrossRef]
278. Cai, Z.; Sun, J.; Shi, L.; Liu, Y.; Wu, X.; Dai, C. An effective method for identifying cow milk powder adulteration levels in goat milk powder using hyperspectral imaging. *J. Food Meas. Charact.* **2025**, *19*, 8854–8868. [CrossRef]
279. Zhang, X.; Huang, X.; Tian, X.; Wang, L.; Dai, C.; Chang, X.; Ren, Y.; Yu, S.; Wang, C.; Han, F. Non-destructive quality monitoring of Shanxi vinegar production during the fumigation stage using computer vision, electronic nose and near-infrared spectroscopy assisted by machine learning. *J. Food Compos. Anal.* **2025**, *146*, 107908. [CrossRef]
280. Adade, S.; Lin, H.; Jiang, H.; Haruna, S.; Barimah, A.; Zareef, M.; Agyekum, A.; Johnson, N.; Hassan, M.; Li, H.; et al. Fraud detection in crude palm oil using SERS combined with chemometrics. *Food Chem.* **2022**, *388*, 132973. [CrossRef] [PubMed]
281. Nirere, A.; Sun, J.; Atindana, V.; Hussain, A.; Zhou, X.; Yao, K. A comparative analysis of hybrid SVM and LS-SVM classification algorithms to identify dried wolfberry fruits quality based on hyperspectral imaging technology. *J. Food Process. Preserv.* **2022**, *46*, e16320. [CrossRef]
282. Kang, W.; Lin, H.; Adade, S.; Wang, Z.; Ouyang, Q.; Chen, Q. Advanced sensing of volatile organic compounds in the fermentation of kombucha tea extract enabled by nano-colorimetric sensor array based on density functional theory. *Food Chem.* **2023**, *405*, 134193. [CrossRef]
283. Ding, Y.; Zeng, R.; Jiang, H.; Guan, X.; Jiang, Q.; Song, Z. Classification of tea quality grades based on hyperspectral imaging spatial information and optimization models. *J. Food Meas. Charact.* **2024**, *18*, 9098–9112. [CrossRef]
284. Li, L.; Xie, S.; Zhu, F.; Ning, J.; Chen, Q.; Zhang, Z. Colorimetric sensor array-based artificial olfactory system for sensing Chinese green tea's quality: A method of fabrication. *Int. J. Food Prop.* **2017**, *20*, 1762–1773. [CrossRef]
285. Li, H.; Zhang, B.; Hu, W.; Liu, Y.; Dong, C.; Chen, Q. Monitoring black tea fermentation using a colorimetric sensor array-based artificial olfaction system. *J. Food Process. Preserv.* **2018**, *42*, e13348. [CrossRef]
286. Zhang, J.; Wu, X.; He, C.; Wu, B.; Zhang, S.; Sun, J. Near-Infrared Spectroscopy Combined with Fuzzy Improved Direct Linear Discriminant Analysis for Nondestructive Discrimination of Chrysanthemum Tea Varieties. *Foods* **2024**, *13*, 1439. [CrossRef] [PubMed]
287. Liang, J.; Wang, Y.; Shi, Y.; Huang, X.; Li, Z.; Zhang, X.; Zou, X.; Shi, J. Non-destructive discrimination of homochromatic foreign materials in cut tobacco based on VIS-NIR hyperspectral imaging. *J. Sci. Food Agric.* **2023**, *103*, 4545–4552. [CrossRef] [PubMed]
288. Ekumah, J.; Adade, S.; Nunekpeku, X.; Zhong, M.; Sun, Y.; Liang, Q.; Virk, M.; Johnson, N.; Kwadzokpui, B.; Ren, X. Nondestructive prediction and classification of gel strength in ethanol-treated kudzu starch gels using near-infrared spectroscopy. *Food Chem.* **2025**, *476*, 143357. [CrossRef] [PubMed]
289. Ouyang, Q.; Wang, L.; Park, B.; Kang, R.; Chen, Q. Simultaneous quantification of chemical constituents in matcha with visible-near infrared hyperspectral imaging technology. *Food Chem.* **2021**, *350*, 129141. [CrossRef] [PubMed]

290. Zhang, Z.; Lu, Y.Z.; Liu, P.F. Training Strategy Optimization of a Tea Canopy Dataset for Variety Identification During the Harvest Period. *Agriculture* **2025**, *15*, 2027. [CrossRef]
291. Li, K.Q.; Chen, T.; Yue, D.Z.; Guo, C.L.; Deng, S.F.; Li, X.L. Early In Ovo Sex Identification of Chicken Embryos Using a Dual-Stage Difference-Enhanced Spectral Fusion Network Based on Visible-Near-Infrared Transmission Spectroscopy. *Animals* **2026**, *16*, 2796. [CrossRef] [PubMed]
292. Paternostre, L.; Baeten, V.; Ampe, B.; Millet, S.; De Boever, J. The usefulness of NIRS calibrations based on feed and feces spectra to predict nutrient content, digestibility and net energy of pig feeds. *Anim. Feed Sci. Technol.* **2021**, *281*, 115091. [CrossRef]
293. Edo, G.; Godana, E.; Ngea, G.; Wang, K.; Yang, Q.; Zhang, H. Improving Biocontrol Potential of Antagonistic Yeasts Against Fungal Pathogen in Postharvest Fruits and Vegetables Through Application of Organic Enhancing Agents. *Foods* **2025**, *14*, 3075. [CrossRef] [PubMed]
294. Alenyorege, E.; Ma, H.; Ayim, I.; Zhou, C. Ultrasound decontamination of pesticides and microorganisms in fruits and vegetables: A review. *J. Food Saf. Food Qual.-Arch. Fur Leb.* **2018**, *69*, 80–91. [CrossRef]
295. Xu, B.; Tiliwa, E.; Yan, W.; Azam, S.; Wei, B.; Zhou, C.; Ma, H.; Bhandari, B. Recent development in high quality drying of fruits and vegetables assisted by ultrasound: A review. *Food Res. Int.* **2022**, *152*, 110744. [CrossRef] [PubMed]
296. Wang, L.; Zhong, H.; Liu, K.; Guo, A.; Qi, X.; Cai, M. The evaluation of kefir pure culture starter: Liquid-core capsule entrapping microorganisms isolated from kefir grains. *Food Sci. Technol. Int.* **2016**, *22*, 598–608. [CrossRef] [PubMed]
297. Godana, E.; Yang, Q.; Wang, K.; Zhang, H.; Zhang, X.; Zhao, L.; Abdelhai, M.; Legrand, N. Bio-control activity of *Pichia anomala* supplemented with chitosan against *Penicillium expansum* in postharvest grapes and its possible inhibition mechanism. *Lwt-Food Sci. Technol.* **2020**, *124*, 109188. [CrossRef]
298. Liang, Z.; Xu, X.; Yang, D.; Liu, Y. The Development of a Lightweight DE-YOLO Model for Detecting Impurities and Broken Rice Grains. *Agriculture* **2025**, *15*, 848. [CrossRef]
299. Navarro-Hortal, M.; Ramírez-Tortosa, C.; Varela-López, A.; Romero-Márquez, J.; Ochoa, J.; Ramírez-Tortosa, M.; Forbes-Hernández, T.; Granados-Principal, S.; Battino, M.; Quiles, J. Heart Histopathology and Mitochondrial Ultrastructure in Aged Rats Fed for 24 Months on Different Unsaturated Fats (Virgin Olive Oil, Sunflower Oil or Fish Oil) and Affected by Different Longevity. *Nutrients* **2019**, *11*, 2390. [CrossRef] [PubMed]
300. Geng, W.; Haruna, S.; Li, H.; Kademi, H.; Chen, Q. A Novel Colorimetric Sensor Array Coupled Multivariate Calibration Analysis for Predicting Freshness in Chicken Meat: A Comparison of Linear and Nonlinear Regression Algorithms. *Foods* **2023**, *12*, 720. [CrossRef] [PubMed]
301. Hao, D.; Tu, X.; Zhang, X.; Guo, S.; Sun, L.; Li, J.; Wang, D.; Xu, W.; Li, P. Effects of proteases inactivation on textural quality of yellow-feathered chicken meat and the possible mechanism based on myofibrillar protein. *Food Control* **2024**, *166*, 110713. [CrossRef]
302. Wang, L.; Gao, E.; Hu, M.; Oladejo, A.; Gong, X.; Wang, J.; Zhong, H. Isolation, identification and screening of high-quality yeast strains for the production of milk beer. *Int. J. Dairy Technol.* **2018**, *71*, 944–953. [CrossRef]
303. Cui, H.; Zhang, C.; Li, C.; Lin, L. Preparation and antibacterial activity of Litsea cubeba essential oil/dandelion polysaccharide nanofiber. *Ind. Crops Prod.* **2019**, *140*, 111739. [CrossRef]
304. Wei, W.; Hu, X.; Hou, Z.; Wang, Y.; Zhu, L. Microbial community structure and diversity in different types of non-bovine milk. *Curr. Opin. Food Sci.* **2021**, *40*, 51–57. [CrossRef]
305. Guo, Y.; Cui, H.; Wang, X.; Guo, H.; Feng, X.; Yan, A.; Pan, Y.; He, L.; Liu, L.; Zhang, K.; et al. Interactions between raw dark tea chemistry and dominant fungi shape Hei brick tea quality. *Int. J. Food Microbiol.* **2025**, *442*, 111364. [CrossRef] [PubMed]
306. Wang, X.; Weng, Z.; Feng, X.; Ye, H.; Lv, H.; Yan, A.; Pan, Y.; Wei, Y.; Chen, T.; He, L.; et al. Blending coffee white tea with flower flavor rooibos to mask the burnt flavor. *Food Chem.* **2025**, *493*, 146058. [CrossRef] [PubMed]
307. Zhou, X.; Wu, X.; Wu, B. Comparative study of indirect and direct feature extraction algorithms in classifying tea varieties using near-infrared spectroscopy. *Curr. Res. Food Sci.* **2025**, *10*, 101065. [CrossRef] [PubMed]
308. Qiu, Z.; Paul, H.; Wang, Z.; Hirai, S.; Kawamura, S. An Evaluation System of Robotic End-Effectors for Food Handling. *Foods* **2023**, *12*, 4062. [CrossRef] [PubMed]
309. Auad, L.; Ginani, V.; Leandro, E.; Stedefeldt, E.; Habu, S.; Nakano, E.; Nunes, A.; Zandonadi, R. Food Trucks: Assessment of an Evaluation Instrument Designed for the Prevention of Foodborne Diseases. *Nutrients* **2019**, *11*, 430. [CrossRef] [PubMed]
310. Roberts, D.; Bahn, V.; Ciuti, S.; Boyce, M.; Elith, J.; Guillera-Arroita, G.; Hauenstein, S.; Lahoz-Monfort, J.; Schröder, B.; Thuiller, W.; et al. Cross-validation strategies for data with temporal, spatial, hierarchical, or phylogenetic structure. *Ecography* **2017**, *40*, 913–929. [CrossRef]
311. Tampu, I.; Eklund, A.; Haj-Hosseini, N. Inflation of test accuracy due to data leakage in deep learning-based classification of OCT images. *Sci. Data* **2022**, *9*, 580. [CrossRef] [PubMed]
312. Steyerberg, E.; Harrell, F. Prediction models need appropriate internal, internal-external, and external validation. *J. Clin. Epidemiol.* **2016**, *69*, 245–247. [CrossRef] [PubMed]

313. Nicolaï, B.; Beullens, K.; Bobelyn, E.; Peirs, A.; Saeys, W.; Theron, K.; Lammertyn, J. Nondestructive measurement of fruit and vegetable quality by means of NIR spectroscopy: A review. *Postharvest Biol. Technol.* **2007**, *46*, 99–118. [CrossRef]
314. Zhang, L.; Small, G.; Arnold, M. Multivariate calibration standardization across instruments for the determination of glucose by Fourier transform near-infrared spectrometry. *Anal. Chem.* **2003**, *75*, 5905–5915. [CrossRef] [PubMed]
315. Mishra, P.; Passos, D. Deep calibration transfer: Transferring deep learning models between infrared spectroscopy instruments. *Infrared Phys. Technol.* **2021**, *117*, 103863. [CrossRef]
316. Jensen, V.; Bianchi, F.; Anfinsen, S. Ensemble Conformalized Quantile Regression for Probabilistic Time Series Forecasting. *IEEE Trans. Neural Netw. Learn. Syst.* **2024**, *35*, 9014–9025. [CrossRef] [PubMed]
317. Selvaraju, R.; Cogswell, M.; Das, A.; Vedantam, R.; Parikh, D.; Batra, D. Grad-CAM: Visual Explanations from Deep Networks via Gradient-Based Localization. *Int. J. Comput. Vis.* **2020**, *128*, 336–359. [CrossRef]
318. Aas, K.; Jullum, M.; Loland, A. Explaining individual predictions when features are dependent: More accurate approximations to Shapley values. *Artif. Intell.* **2021**, *298*, 103502. [CrossRef]
319. Kapoor, S.; Cantrell, E.; Peng, K.; Pham, T.; Bail, C.; Gundersen, O.; Hofman, J.; Hullman, J.; Lones, M.; Malik, M.; et al. REFORMS: Consensus-based Recommendations for Machine-learning-based Science. *Sci. Adv.* **2024**, *10*, eadk3452. [CrossRef] [PubMed]
320. Pineau, J.; Vincent-Lamarre, P.; Sinha, K.; Larivière, V.; Beygelzimer, A.; d'Alché-Buc, F.; Fox, E.; Larochelle, H. Improving Reproducibility in Machine Learning Research (A Report from the NeurIPS 2019 Reproducibility Program). *J. Mach. Learn. Res.* **2021**, *22*, 1–20.
321. Rong, Y.; Zareef, M.; Liu, L.; Din, Z.; Chen, Q.; Ouyang, Q. Application of portable Vis-NIR spectroscopy for rapid detection of myoglobin in frozen pork. *Meat Sci.* **2023**, *201*, 109170. [CrossRef] [PubMed]
322. Hu, Y.; Sheng, W.; Adade, S.; Wang, J.; Li, H.; Chen, Q. Comparison of machine learning and deep learning models for detecting quality components of vine tea using smartphone-based portable near-infrared device. *Food Control* **2025**, *174*, 111244. [CrossRef]
323. Bilal, M.; Arslan, M.; Samee-Ullah; Shishir, M.; Shaukat, F.; Li, Z.; Xia, S.; Xiaobo, Z. Efficient detection of adulteration in peanut seed oil using a smartphone-based colorimetric sensor array system. *J. Food Compos. Anal.* **2025**, *144*, 107654. [CrossRef]
324. Sun, J.; Xin, X.; Xin, Y.; Cong, S. Non-destructive identification of processing methods of Yunnan coffee beans via portable near-infrared spectrometer and lightweight MobileNetV4. *J. Food Compos. Anal.* **2026**, *149*, 108724. [CrossRef]
325. Yin, L.; Ma, L.; Jia, W.; Gong, Y.; Cai, J. Portable SERS-based lateral flow strip for simultaneous rapid detection of three typical corn mycotoxins. *Food Chem.* **2026**, *502*, 147677. [CrossRef] [PubMed]
326. Zhu, J.; Qian, H.; Zhu, A.; Xu, Y.; Zhao, S.; Wei, W.; Chen, Q. Rapid and non-destructive determination of acidity and peroxide index of extra virgin olive oil using portable near-infrared spectroscopy and a novel chemometric approach. *J. Food Compos. Anal.* **2025**, *146*, 107900. [CrossRef]
327. Wu, Y.; Zhang, J.; Hu, X.; Huang, X.; Zhang, X.; Zou, X.; Shi, J. A visible colorimetric sensor array based on chemo-responsive dyes and chemometric algorithms for real-time potato quality monitoring systems. *Food Chem.* **2023**, *405*, 134717. [CrossRef] [PubMed]
328. Yan, J.K.; Wang, Y.Y.; Qiu, W.Y.; Ma, H.L.; Wang, Z.B.; Wu, J.Y. Three-phase partitioning as an elegant and versatile platform applied to nonchromatographic bioseparation processes. *Crit. Rev. Food Sci. Nutr.* **2018**, *58*, 2416–2431. [CrossRef] [PubMed]
329. Xin, X.; Sun, J.; Shi, L.; Yao, K.; Zhang, B. Application of hyperspectral imaging technology combined with ECA-MobileNetV3 in identifying different processing methods of Yunnan coffee beans. *J. Food Compos. Anal.* **2025**, *143*, 107625. [CrossRef]
330. Kurdthongmee, W.; Sukkuea, A. Non-Destructive Volume Estimation of Oranges for Factory Quality Control Using Computer Vision and Ensemble Machine Learning. *J. Imaging* **2025**, *11*, 352. [CrossRef] [PubMed]
331. Xu, Q.; Cai, J.R.; Zhang, W.; Bai, J.W.; Li, Z.Q.; Tan, B.; Sun, L. Detection of citrus Huanglongbing (HLB) based on the HLB-induced leaf starch accumulation using a home-made computer vision system. *Biosyst. Eng.* **2022**, *218*, 163–174. [CrossRef]
332. Wu, X.H.; Yang, Z.T.; Yang, Y.L.; Wu, B.; Sun, J. Geographical Origin Identification of Chinese Red Jujube Using Near-Infrared Spectroscopy and Adaboost-CLDA. *Foods* **2025**, *14*, 803. [CrossRef] [PubMed]
333. Chen, Z.J.; Zhang, G.Y.; Zhang, F. Multimodal AI for Real-Time Food Safety and Quality: From Sensors to Foundation Models, Edge Deployment, and Regulation. *Food Sci. Nutr.* **2026**, *14*, e71534. [CrossRef] [PubMed]
334. Arslan, M.; Tahir, H.; Zareef, M.; Shi, J.; Rakha, A.; Bilal, M.; Huang, X.; Li, Z.; Zou, X. Recent trends in quality control, discrimination and authentication of alcoholic beverages using nondestructive instrumental techniques. *Trends Food Sci. Technol.* **2021**, *107*, 80–113. [CrossRef]
335. Pan, X.; Yang, S.; Gao, Y.; Wang, Z.; Zhai, C.; Qiu, W. Evaluation of Spray Drift from an Electric Boom Sprayer: Impact of Boom Height and Nozzle Type. *Agronomy* **2025**, *15*, 160. [CrossRef]
336. Zhang, L.; Zhang, H.; Zhu, Q.; Niu, Y. Further investigating the performance of crop water stress index for maize from baseline fluctuation, effects of environmental factors, and variation of critical value. *Agric. Water Manag.* **2023**, *285*, 108349. [CrossRef]
337. Wang, J.; Ahmad, W.; Hassan, M.; Zareef, M.; Viswadevarayalu, A.; Arslan, M.; Li, H.; Chen, Q. Landing microextraction sediment phase onto surface enhanced Raman scattering to enhance sensitivity and selectivity for chromium speciation in food and environmental samples. *Food Chem.* **2020**, *323*, 126812. [CrossRef] [PubMed]

338. Tang, N.; Sun, J.; Yao, K.; Zhou, X.; Tian, Y.; Cao, Y.; Nirere, A. Identification of *Lycium barbarum* varieties based on hyperspectral imaging technique and competitive adaptive reweighted sampling-whale optimization algorithm-support vector machine. *J. Food Process. Eng.* **2020**, *44*, 13603. [CrossRef]
339. Zhu, L.; Cheng, M.; Xu, C.; Wang, R.; Zhang, M.; Tao, Y.; Qi, S.; Wei, W. Selective Inactivation Strategies for Vegetable Raw Materials: Regulating Microbial Communities to Ensure the Safety and Quality of Fermented Vegetables. *Foods* **2025**, *14*, 3291. [CrossRef] [PubMed]
340. Zhang, J.; Hamadou, A.; Qi, Y.; Chen, Z.; Yue, L.; Xu, B. Updated insights into designing bioactive compounds-loaded protein-based nanoparticles using pH-driven method: Positive impacts of technical evolutions based on existing theoretical framework. *Food Chem.* **2026**, *505*, 148089. [CrossRef] [PubMed]
341. Wu, H.; Li, X.; Lu, H.; Tong, L.; Kang, S. Crop acreage planning for economy- resource- efficiency coordination: Grey information entropy based uncertain model. *Agric. Water Manag.* **2023**, *289*, 108557. [CrossRef]
342. Zhang, X.N.; Huang, X.Y.; Wang, Z.L.; Zhang, Y.; Huang, X.W.; Li, Z.H.; Daglia, M.; Xiao, J.B.; Shi, J.Y.; Zou, X.B. Bioinspired nanozyme enabling glucometer readout for portable monitoring of pesticide under resource-scarce environments. *Chem. Eng. J.* **2022**, *429*, 132243. [CrossRef]
343. Gunning, Y.; Taous, F.; El Ghali, T.; Gibbon, J.D.; Wilson, E.; Brignall, R.M.; Kemsley, E.K. Mitigating instrument effects in 60 MHz 1H NMR spectroscopy for authenticity screening of edible oils. *Food Chem.* **2022**, *370*, 131333. [CrossRef] [PubMed]
344. Bernat, A.; Samiwala, M.; Albo, J.; Jiang, X.Y.; Rao, Q.C. Challenges in SERS-based pesticide detection and plausible solutions. *J. Agric. Food. Chem.* **2019**, *67*, 12341–12347. [CrossRef] [PubMed]
345. Chai, X.Y.; Hu, J.P.; Ma, T.L.; Liu, P.; Shi, M.L.; Zhu, L.J.; Zhang, M.; Xu, L.Z. Construction and Characteristic Analysis of Dynamic Stress Coupling Simulation Models for the Attitude-Adjustable Chassis of a Combine Harvester. *Agronomy* **2024**, *14*, 1874. [CrossRef]

Disclaimer/Publisher's Note: The statements, opinions and data contained in all publications are solely those of the individual author(s) and contributor(s) and not of MDPI and/or the editor(s). MDPI and/or the editor(s) disclaim responsibility for any injury to people or property resulting from any ideas, methods, instructions or products referred to in the content.